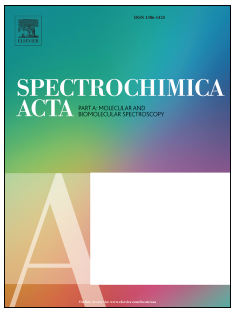

The specific binding of a new 1,2,3-triazole to three blood proteins and it's appended rhodamine complex for selective detection of Hg^{2+}

Guohua Ding, Luyong Wu, Huajie Feng, Yanping Liu, Jianling Li, Hongzong Si, Xiaojun Yao, Mengxiong He, Wenying He

PII: S1386-1425(19)31118-7

DOI: https://doi.org/10.1016/j.saa.2019.117728

Reference: SAA 117728

To appear in: *Spectrochimica Acta Part A: Molecular and Biomolecular Spectroscopy*

Received Date: 30 June 2019

Revised Date: 26 October 2019

Accepted Date: 28 October 2019

Please cite this article as: G. Ding, L. Wu, H. Feng, Y. Liu, J. Li, H. Si, X. Yao, M. He, W. He, The specific binding of a new 1,2,3-triazole to three blood proteins and it's appended rhodamine complex for selective detection of Hg^{2+}, *Spectrochimica Acta Part A: Molecular and Biomolecular Spectroscopy* (2019), doi: https://doi.org/10.1016/j.saa.2019.117728.

The specific binding of a new 1,2,3-triazole to three blood proteins and it's appended rhodamine complex for selective detection of Hg^{2+}

Guohua Ding[a], Luyong Wu[a], Huajie Feng[a], Yanping Liu[a], Jianling Li[a], Hongzong Si [b], Xiaojun Yao[c], Mengxiong He [a] , Wenying He [a]*

[a] *Key Laboratory of Tropical Medicinal Resource Chemistry of Ministry of Education, Hainan Normal University, 571158 Haikou, China*

[b] *Institute for Computational Science and Engineering, Qingdao University, 266071 Qingdao, China*

[c] *College of Chemical and Chemical Engineering, Lanzhou University, 730000 Lanzhou, China*

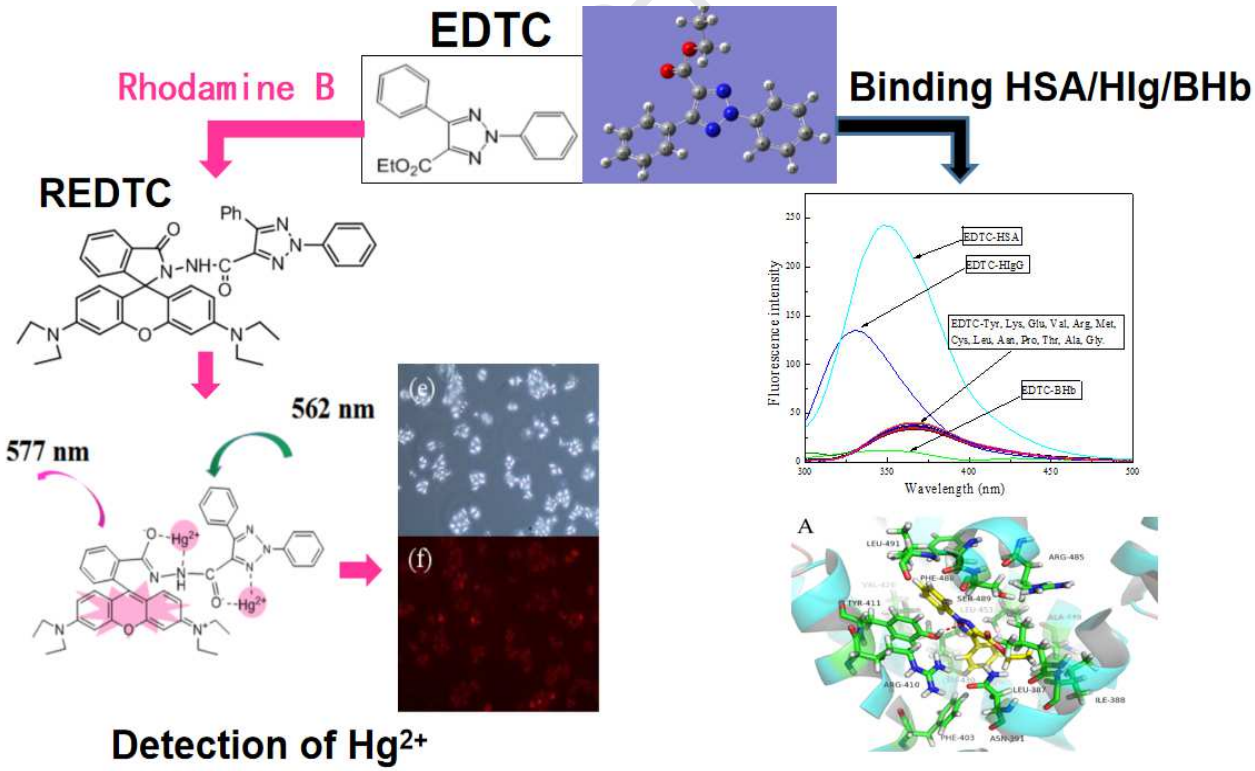

*Corresponding author at: Key Laboratory of Tropical Medicinal Resource Chemistry of Ministry of Education, Hainan Normal University, Hainan Normal University, Haikou 571158, China.
E-mail address: hewenying@hainnu.edu.cn(WY He)

The specific binding of a new 1,2,3-triazole to three blood proteins and it's appended rhodamine complex for selective detection of Hg^{2+}

Guohua Ding[a], Luyong Wu[a], Huajie Feng[a], Yanping Liu[a], Jianling Li[a], Hongzong Si[b], Xiaojun Yao[c], Mengxiong He[a], Wenying He[a]*

[a] *Key Laboratory of Tropical Medicinal Resource Chemistry of Ministry of Education, Hainan Normal University, 571158 Haikou, China*

[b] *Institute for Computational Science and Engineering, Qingdao University, 266071 Qingdao, China*

[c] *College of Chemical and Chemical Engineering, Lanzhou University, 730000 Lanzhou, China*

ABSTRACT

A synthesized compound, ethyl 2,5-diphenyl-2H-1,2,3-triazole-4- carboxylate (EDTC) was investigated on its physiochemical parameters and structural properties by using the quantum-chemical method. The results on the theoretical spectrum of EDTC were line with experimental fluorescence and absorption spectrum in large degree. Then EDTC was successfully synthesized to a novel rhodamine-based fluorescent probe (REDTC), which showed a distinct fluorescence enhancement upon the presence of Hg^{2+} in dimethyl formamide-water (DMF-H_2O) buffer solution (pH 7.4). Meanwhile, the triazole appended colorless compound turns to pink upon complex formation with Hg^{2+} ions as 1:2 molar ratios and enables naked-eye detection. The chromogenic mechanism was determined by using spectroscopic measurements and TD DFT calculation. The fluorescence imaging

*Corresponding author at: Key Laboratory of Tropical Medicinal Resource Chemistry of Ministry of Education, Hainan Normal University, Hainan Normal University, Haikou 571158, China.
E-mail address: hewenying@hainnu.edu.cn(WY He)

experiments of Hg^{2+} in HeLa cell revealed that the probe REDTC could be labeled and it could be used in biological systems. Also, the intermediate EDTC was developed as a sensitive fluorescent probe for specific studies on the interactions to three kinds of blood proteins including human serum albumin (HSA), human immunoglobulin (HIg) and bovine hemoglobin (BHb) by using a series of spectroscopic methods and molecular docking under the simulative physiological conditions. The interactions between EDTC and these proteins led to the distinct fluorescence enhancement. The thermodynamic measured results further suggested that hydrophobic forces play a dominating role in stabilizing the complexes, which are in correspondence with the results from molecular docking. The UV-visible, synchronous, and three-dimensional (3D) fluorescence measurements demonstrated that EDTC influences the conformational of proteins and the microenvironment surrounding HSA, HIg, or BHb in aqueous solution.

Keywords: ethyl 2,5-diphenyl-2H-1, 2, 3-triazole-4-carboxylate; structural properties; Hg^{2+} ions; binding; blood protein.

1. Introduction

Since the representative research on the Cu(I)-catalyzed azide-alkyne cycloaddition reaction for the synthesis of 1,2,3-triazole in 2002[1], this organic reaction as the so-called click chemistry has been widely applied in various fields of biological, chemical, macromlecualr materials and pharmaceutical sciences due to its manifold chemical versatility and orthogonality[2]. 1,2,3-triazoles, a class of five-membered nitrogen heterocycles manifest a privileged structural component in a great variety of bioactive molecules, which have recently been well investigated on account of their low toxic effects and several pharmacological properties[3]. They can

also act as ligands capable of binding to various metal ions. Therefore, it is very important to prepare novel 1,2,3-triazole derivatives with various functional substituents in order to discovery compounds possessing coordination ability to different transition metals as well as new types of biological activity[4,5,6]. Among the various probes of detecting metal ions, rhodamine-based fluorescent probes have a time-honored role due to their excellent spectroscopic properties, such as long absorption, large extinction coefficient and emission wavelength, high fluorescence quantum yield, and high light stability[7]. Up to now, several fluorescence probes based on triazole-rhodamine complexes have also been reported and can be applied to detect specific metal ions [8-10].

It is well known that heavy metal pollution is widespread and be derived from extensive natural and anthropogenic sources, which can threat to the humanity's life even at low concentrations because of the accumulative and toxic properties. As one of the most prevalent toxic heavy metals, mercury, or mercury ion (Hg^{2+}) is considerably harmful to the environment and the human body. Excessive intake of mercury accumulation will cause multitudinous chronic diseases such as headache, deafness, visual impairment, central nervous system, and even irreversible damage of the brain. Therefore, developing a highly selective and rapid method for detecting mercury ions is still a vital need in order to solve the problem of increasingly urgent mercury pollution in water and the environment. Above all, the colorimetric sensors have drawn greater attention due to the advantages of fast response, signal visibility, and application for on-site and high throughput measurement[11-12]. In present work, ethyl 2,5-diphenyl-2H-1,2,3-triazole-4-carboxylate (EDTC, Scheme 1) was a new compound[13] and introduced to rhodamine B to synthesize a novel derivative named REDTC, which exhibited excellent selectivity toward Hg^{2+} with chromogenic reaction

over other metal ions.

On the other hand, given the biological significance of the l, 2, 3-triazoles, recent studies have revealed that 1, 2, 3-triazole moieties and related heterocyclic compounds have been identified as bioactive molecules, and occupied a prominent field in medicinal chemistry because of their therapeutic properties and favorable metabolic stability. Thus, their drug-like properties have been developed and made full use in medicinal chemistry[2]. It is a well-known face that proteins are frequently the ‘targets’ for therapeutically active pharmaceuticals of both synthetic and natural origin[14]. The blood proteins serve on the shipping object for small molecule drugs, and the bonding interaction between drugs and protein has a great impact on the distribution of these drugs in the body and the corresponding model of metabolism and excretion. So it is an important research area on the binding properties of small molecule drugs to plasma proteins.

Among of various target proteins, three kinds of blood proteins including human serum albumin (HSA), human immunoglobulin (HIg) and bovine hemoglobin (BHb) were usually applied to as plasma model proteins[15]. As one of the model blood protein, HSA is the most abundant multifunctional protein and takes up large proportion of the total protein content of plasma. It plays a vital role in transporting and depositing several exogenous and endogenous substances including dyes, hormones, fatty acids, and numerous drugs in the blood stream to the related target organ [16]. The second model protein is HIg, which involved in different cell actions and human immune response. It is usually used as the biomarker of numerous diseases such as cancers, liver disease, Alzheimer's disease, inflammatory bowel disease, infectious disease and autoimmune disease, etc [17]. As the third model protein, hemoglobin (Hb) is also one of the major functional proteins in the vascular

system of animals. It belongs to an iron-containing metalloprotein and responsible for the transportation of oxygen in blood red cells. The changes in the abnormally high or low amount of Hb in human serum can cause some possible healthy problems, such as anemia and polycythemia[18]. The above three kinds of model proteins are widespread used in biochemical and biophysical researches on the bonding interactions between proteins and small molecules [15, 17,18]. The various spectroscopic techniques have become more valuable methods to study these interactions at the molecular level in consideration of the advantages of rapidness, sensitivity, convenience, and high simplicity[19]. However, many types of research are based on the phenomenon of fluorescence quenching of proteins by small molecular drugs and thus led to the second structure changes of these biomacromolecules [20-21]. In the present paper, it is interesting that we reported a new array on the interaction of EDTC with three blood proteins by the fluorescence enhancement.

In short, we designed and synthesized a novel rhodamine B derivative REDTC by using EDTC and rhodamine B, which shown a distinct chromogenic reaction with Hg^{2+} over than other metal ions originated the opening of the spironolactone ring. Then the structural properties and physiochemical parameters of EDTC were studied by quantum-chemical methods. Finally, based on the fluorescence enhancement mechanism, as a special probe, EDTC was used to study the interaction to HSA, HIg and BHb by fluorescence spectroscopy, UV/vis absorption spectroscopy and molecular modeling methods. These results are the first spectroscopic application and bioactivity results on EDTC or REDTC at the molecular level, which can illustrate the nature of EDTC or REDTC information for further exploitation.

2. Materials and Methods

2.1. Materials and apparatus

EDTC was provided by Organic Chemistry Laboratory of Hainan Normal University, China, and the stock solution (1.0×10^{-3} mol /L) was prepared in methanol. Both of blood proteins, including HSA(10 g/50 mL) and HIg(2.5g/50 mL) were purchased from Shanghai Bio Science & Technology Co. BHb(solid) was purchased from Worthington Biochemical Corporation. All protein stock solutions were dissolved in 20 mM, Tris-HCl buffer pH 7.4, and the concentration is 3.0×10^{-5} mol /L. Sodium hydroxide (NaOH) and chloride salts including Al^{3+}, Pb^{2+}, Mg^{2+}, Mn^{2+}, Hg^{2+}, Fe^{3+}, Zn^{2+}, Mo^{2+}, Cd^{2+}, Cu^{2+}, Na^{+}, Ni^{2+}, Co^{2+} , Ca^{2+} , $K^{+}$and Ag^{+}, and were acquired from Sinopharm Chemical Reagent Co., Ltd (Shanghai, China). All other reagents were of analytical reagent grade and obtained commercially without further purification. Doubly distilled water was used throughout the experiment.

NMR spectra were measured on a Bruker Avance 400MHz spectrometer at room temperature. Fluorescent spectra were obtained by using an RF-5301PC spectrofluoro photometer (Shimadzu, Japan) equipped with a xenon lamp source and a water bath. UV-vis absorption spectra were recorded on a Hitachi U3900/3900H spectrophotometer (Hitachi, Japan) equipped with 1.0 cm quartz cells. The 3D fluorescence spectra were recorded on an F-7000 spectrofluorophotometer (Hitachi, Japan). The pH measurement was performed on a PHS-3C pH meter (Shanghai, China).

2.2 Synthesis

As shown in Scheme S1, the first step is to synthesize rhodamine B hydrazide **1** according to the literature [22]. Rhodamine B (1.0 g, 2.1 mmol) was dissolved in 20 mL ethanol in a 50mL flask, 80% hydrazine hydrate (2 mL) was then added with stirring at room temperature and the stirred mixture was heated to reflux for 3 h . Then

water (50 mL) added to the mixture was extracted with ethyl acetate (50 mL) three times. The combined organic layer was dried over anhydrous sodium sulfate and then filtered, affording intermediate **1** as a yellow solid (0.52 g, 54.74%); ^{1}H NMR (400 MHz, $CDCl_3$):δ (ppm) = 1.16 (t, J = 6.8 Hz, 12H),3.34 (q, J = 7.2 Hz, 8H), 3.61 (s, 2H), 6.30 (m, 2H), 6.45(m, 4H), 7.1 (m, J = 2.64 Hz, 1H), 7.44 (m, 2H), 7.94(m, 1H); ^{13}CNMR (400 MHz, $CDCl_3$) δ (ppm) = 166.03, 153.75, 151.45, 148,78,132.39, 129.91, 128.00, 127.95, 123.71, 122.83, 107.94, 104.47, 97.89, 77.32, 77.00, 76.68, 65.82, 44.25, 12.50.

The second step is a synthesis of REDTC as follows: A mixture of EDTC (100 mg, 0.34 mmol), and potassium hydroxide (100 mg, 1.79 mmol) in 10 mL of a 1:1 mixture of ethanol: water was stirred for four hours, then heated to reflux for two hours. After cooling to room temperature, hydrochloric acid was added dropwise with stirring until the pH of the solution was below 1. The mixture was poured into water and extracted with ethyl acetate. The organic phase was washed three times with water and dried over Na_2SO_4. The solvent was removed by evaporation, affording a solid of 2.3mL $SOCl_2$ was added to the flask of compound **2,** and the reaction mixture was refluxed for three hours at 90□. Then the residuary $SOCl_2$ was distilled out and obtained the residue **3**. The residue **3** was dissolved in 10 mL dichloromethane and was mixed with intermediate **1** (150mg, 0.33mmol) and 1 mL triethylamine. The mixture was stirred at room temperature for 12h then extracted with ethyl acetate. After drying, the crude product was purified on a silica column using petroleum ether: ethyl acetate (3:1, v/v) as the eluent to afford product REDTC (148.7 mg,61.98%). ^{1}H NMR (400 MHz, $CDCl_3$):δ (ppm) = 1.36 (t, *J* = 7.2 Hz, 12H),3.34 (q, *J* = 7.2 Hz, 8H), 6.37 (m, 3H), 6.77 (m, 2H), 7.32(m, 1H), 7.35 (m, 4H), 7.45 (m,2H), 7.53(m,2H), 7.52 (m,2H), 7.84(m,3H), 7.87 (m, 1H); ^{13}CNMR (100 MHz, CDCl3) δ(ppm) =

171.07, 164.97, 158.32, 153.82, 151.18, 149.44, 148.93, 138.96, 137.32, 133.15, 129.46, 129.34, 129.20, 129.04, 129.01, 128.78, 128.33,128.25, 128.02, 124.13, 123.51, 119.18, 107.99, 104.44, 97.59, 77.32, 77.00, 76.68, 66.32, 60.31, 44.31, 29.62, 20.96, 14.12, 12.53. HR-MS (ESI) calcd.for $[M+H]^+$ 704.3349 , found 704.3348.

2.3 *Quantum chemical calculation of EDTC*

The molecular structure of EDTC in the ground state was fully optimized by using GaussView5.0 program package at Hartree-Fock Restricted algorithm level. The Configuration Interaction with Single excitations (CIS) method was carried out to fully optimize the configurations of the lowest excited state. The molecular orbital of EDTC was analyzed by HF/6-31G (d) method. The theoretical absorption spectra and fluorescence emission spectra of EDTC was calculated by using the time-dependent density functional theory (TD DFT). Then the values of electron affinity and ionization potential of EDTC were obtained by Gaussian 09 software at the DFT//B3LYP/6-31G* algorithm level [23]. Also, based on Gaussian 09 program package, B3LYP method was applied to fully optimize the molecular structure of REDTC and calculate the structural energy in terms of LANL2TZ basis set for Hg and 6-311G (d) basis set for H, C, N, O, and F respectively [24].

2.4 General fluorescence spectra and UV-vis measurements on REDTC

The solutions of REDTC and Hg^{2+} of different concentrations were prepared by stepwise dilution of a concentrated stock solution (0.5 mM for REDTC and 5 mM for Hg^{2+}) in acetonitrile and water, respectively. The spectral analyses were carried out in DMF-H_2O buffered (Tris-HCl, v/v, 2/8, pH 7.40) solution at room temperature. The concentration of REDTC for fluorescence and UV-vis measurement was 1×10^{-5} mol /L. The solutions of different metal ions were prepared with chloride salts in water solution. Fluorescence and UV-vis spectrophotometric titrations were done by

successive addition of corresponding chemical reagent using a microliter syringe. To evaluate the selectivity of REDTC for detection of Hg^{2+}, a series of competitive metal ions, including Pb^{2+}, Mn^{2+}, K^{+}, Na^{+}, Ag^{+}, Ca^{2+}, Cd^{2+}, Co^{2+}, Cu^{2+}, Fe^{3+}, Zn^{2+}, Ni^{2+}, Hg^{2+}, Li^{+} and Mg^{2+}, at a final concentration of 500 nM, were tested following the identical experimental procedure.

2.5 Cell culture and fluorescence imaging

HeLa cells were cultured on a 6-well plate with a density of 2×10^{3} cells per well in cell incubator at 37□ with a humidified atmosphere for 12 h before staining. After removing culture media, cells were additionally washed with PBS buffer three times. Then HeLa cells were incubated with chemosensor REDTC(10μM) in the culture media containing ethanol for 30 min at 37□. Experiments to assess Hg^{2+} uptake were performed in the same culture media supplemented with 25 μM Hg^{2+} for 30 min. Moreover, the fluorescence images were acquired through fluorescence microscopy.

2.6 Analytical procedure of the interaction of EDTC with three proteins

Fluorescence measurements: The stock solutions of HSA, HIg, and BHb were diluted to 5 μM, 5μM, and 6×10^{-7} mol/L respectively. The intrinsic fluorescence studies were done in a 1 cm path length cuvette. The HSA/HIg /BHb alone and in the presence of EDTC samples were excited at 278 nm, and emissions were taken in the range of 280 to 500 nm. The test solutions containing 0.05 mol /L Tris-HCl buffer (pH 7.40) and HSA/HIg /BHb solution were titrated by successive additions of 1.0×10^{-4} mol /L EDTC, respectively. Moreover, the excitation and emission slit width was set 5 nm for HSA and BHb while 10 nm for HIg. All fluorescence spectra were measured at three temperatures (300 K, 310 K, and 320 K), which were kept by recycling water throughout the experiment. The synchronous fluorescence spectra were tested by a constant scanning interval Δλ of 15nm and 60nm under the same

concentration condition at room temperature.

3D fluorescence measurements: The stock concentration of EDTC, BHb, HSA and HIg were 1.0×10^{-4} mol /L, 5 μM, 2×10^{-7} mol /L, and 1×10^{-7} mol /L respectively. The 3D emission spectra of three kinds of blood proteins in the absence and presence of EDTC were recorded at the exiting wavelength ranging from 200 to 350 nm and the emission wavelength ranging from 200 to 700 nm. The excitation and emission slit widths were set 5 nm.

UV-vis absorption measurements: The UV-vis absorption spectra of free HSA(4×10^{-7} mol /L), HIg(1×10^{-7} mol /L) and BHb(2×10^{-7} mol /L) in the absence and presence of increasing amount of EDTC were performed at the wavelength range of 200-600 nm in a pH 7.4 tris-HCl buffer solution at room temperature. The absorbance titrations were performed by varying the concentrations of EDTC (0-11.67 μM for HSA, 0-20 μM for HIg and 0-10 μM for BHb，respectively).

Molecular docking: The crystal structure of HSA (PDB ID: 5ID7), HIg (PDB ID: 5DZN), and BHb (PDB ID: 3WHM) were obtained from the Protein Data Bank. The three-dimensional structure of the EDTC molecule was constructed in SYBYL software. The credible binding modes were computed by using SurflexDock program in SYBYL 7.3 software as follows: The polar hydrogen atoms were added, and the structure of water molecules were removed from the crystal structure. Then the docking simulations were initiated by SYBYL software. Then a binding pocket was established by introducing the Kollman-all atom charges to protein atoms, and EDTC molecule was docked into the prepared protein. Finally, Surflex-Dock produced the top 20 options of binding conformation for each ligand ranked by total scores [23].

3. Results and discussion

3.1 The structural and photochemical properties of EDTC

Generally, Frontier Molecular Orbitals (FMO's) including the highest occupied molecular orbital (HOMO) and lowest unoccupied molecular orbital (LUMO) are both of the most important tools used in quantum chemistry. Based on FMO's theory, the interaction between HOMO and LUMO levels of the reacting species results in the formation of a transition state. Moreover, the higher the LUMO energy shows the harder the acceptance of electrons from electron-donating substitutes [25]. Fig. S1 (A) showed the calculated ground-state geometry optimization of EDTC by GaussView5.0 software at the Hartree-Fock Restricted algorithm level, which displayed that the structure of EDTC is nonplanar. The compound EDTC consists of 37 atoms, and the geometrical parameters of EDTC including bond length, bond angle and dihedrals are listed in Table S1 (as shown in Supplemental Materials) by using HF/6-31G(d), CIS/6-31G(d), and B3LYP/6-31G(d) basis sets respectively. From Table S1, it can be seen that the calculated values of bond lengths and bond angles are semblable at these three levels of calculations in great degree. The range of bond length is between 1.07 Å and 2.39 Å, and that of the bond angle varied from 90.70 to 157.85°. However, the dihedrals seem somewhat different given using various computing methods. It is noticeable, the C-C bond lengths in two benzene rings (Tag C6-C17) are between 1.36 and 1.48 Å at three levels, revealing that bonds are longer than the C=C double bond (1.34 Å), but much shorter than the typical C-C single bond (1.54 Å) and some bonds are shorter than that of normal C-N bond (1.47 Å)[26]. These information further confirmed that the molecular structure of EDTC is no planar.

Fig. S1 (B-1) and Fig. 1 (B-2) showed LUMO and HOMO of EDTC, respectively. The calculated value of LUMO (-0.0675eV) is higher than that of

HOMO (-0.2402eV), which suggested that EDTC has weaker ability to accept electrons from other electron donating group. Simultaneously, some physicochemical parameters were also calculated by the diffuse functions B3LYP/6-311G+ (d) at the DFT//B3LYP/6-31G* algorithm level such as adiabatic ionization potential (6.2688eV), vertical ionization potential (6.458 eV), vertical electron affifinity (2.0962eV) and adiabatic electron affinity (2.7231eV) respectively. These values revealed that it is easy for EDTC to lose an electron or the electron accepting the ability of EDTC is very weak [27].

Usually, the HOMO-LUMO gap is an important indicator related to the luminescent properties [28]. The present computed parameters indicated that the electron transition of EDTC focused primarily on HOMO→LUMO transition, suggesting that EDTC had luminescent properties and confirmed by the experimental spectra as followings. Fig. (1A) is the predicted electronic absorption spectra of EDTC by time-dependent DFT (TD-DFT) calculations. The corresponding UV-vis absorption spectra of EDTC in methanol were showed in the inset of Fig. 1(A). We can see that both of the two graphs have the semblable profiles with double peak, but there is some difference in the position of their maximum absorption peaks. Nevertheless it is noted that the second biggest absorption peak is at 286 nm, which is very close to that of the experimental measurement (283 nm). It is reported that the absorption peak observed at about 280 nm was likely due to π-π^* transition and the formation of polyene π bonds by one triazole ring and two benzene rings of EDTC [29]. Fig. 1 (B) is the calculated fluorescence emission spectra of EDTC by TD DFT and those experimented in methanol (illustration in Fig. 1(B)). The position of the maximum fluorescence emission peak is located at 374 nm for the calculated theoretical spectra and 350 nm for the corresponding measured spectra, respectively.

The reasonable excuse about the distinction is that the conjugated aromatic compound EDTC caused π→π* transition from the ground state to the excited state. In general, the polarity of the ground state is weaker than that of the excited state, and low polar solvent can have more impact on stabilizing the ground state. So it led to the shift the position of maximum fluorescence emission towards the longer wavelength side [30]. Herein, As a high polar molecule, methanol is used as a solvent of EDTC and therefore resulted in the blue-shift effect with the maximum fluorescence emission peak from 374 nm to 350 nm.

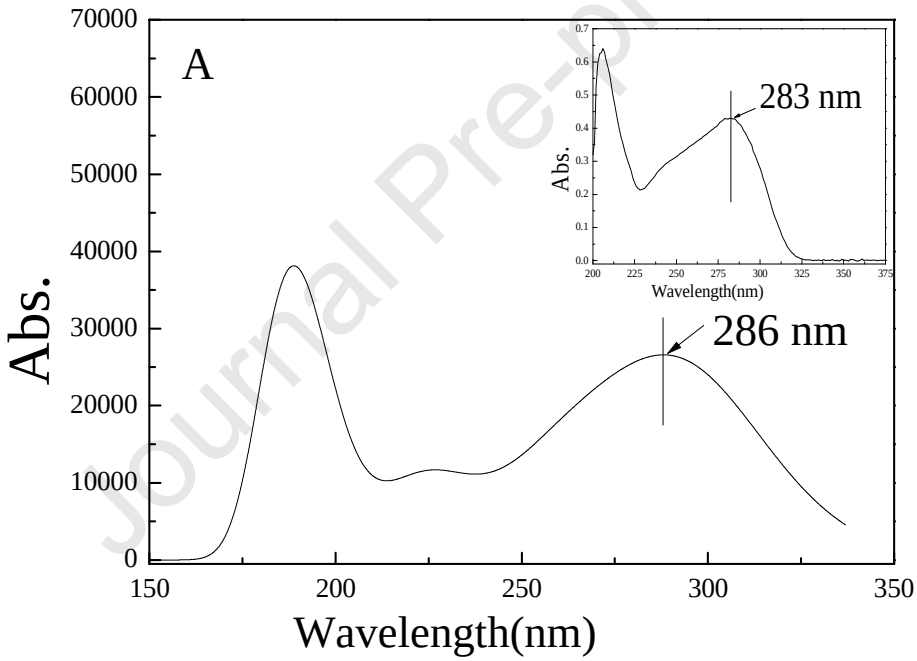

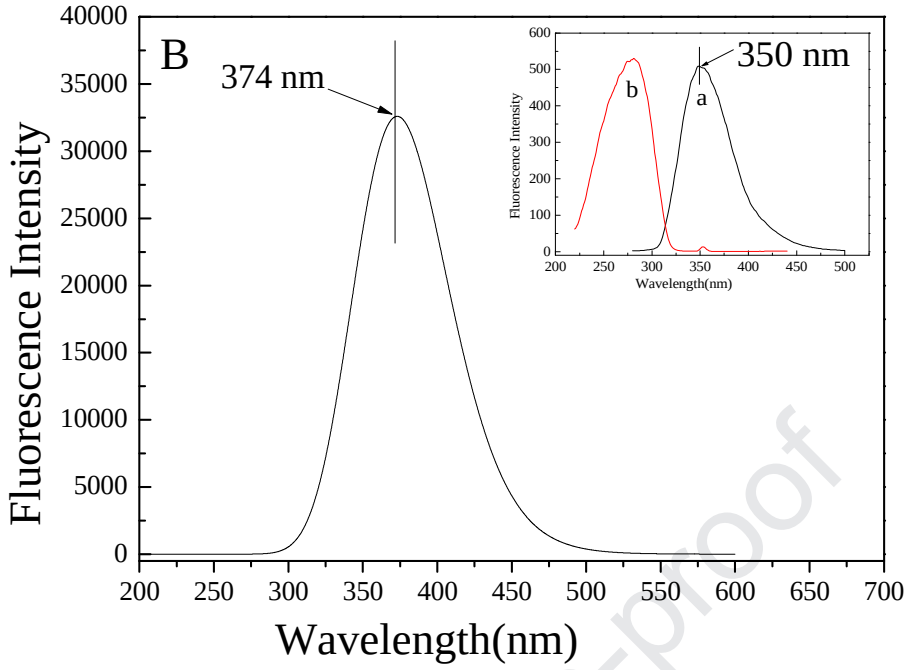

Fig. 1 (A) The electronic absorption spectra of EDTC predicted by TD-DFT calculations. Inset: the absorption spectra of EDTC measured in methanol. (B) The fluorescence emission spectra of EDTC predicted by TD-DFT calculations. Inset: the fluorescence emission spectra of EDTC measured in methanol.

Based on the above results on the UV-Vis absorption and fluorescence spectra, it proclaimed that the computed results are consistent with the experiment results to a great extent. Taking into account the characteristic structure of EDTC, it is inferred that EDTC should have larger fluorescence quantum efficiency because of it is fluorescent emission peak at 350 nm and is an expectant blue light emitting material in the field of organic light-emitting diodes [31].

3.2 Synthesis and spectroscopic characterization of REDTC

A number of highly selective chemosensors for the detection of various metal ions (such as Cu^{2+}, Cd^{2+}, Fe^{3+}, Zn^{2+} and Hg^{2+} etc) based on click produced triazole have been applied and designed [32-35]. Theoretically, given the triazole unit containing ester group, it is possible and feasible for EDTC to synthesize with

rhodamine B hydrazide[36]. So EDTC was explored and synthesized with the rhodamine hydrazide to successfully produce a new rhodamine B derivative REDTC by a serious of synthetic reaction (Scheme S1). REDTC were characterized by ^{1}HNMR(Fig. S2), ^{13}C NMR(Fig. S3), and HRMS(Fig. S4) respectively.

The spectral signature of REDTC was investigated by UV-visible absorption and fluorescence measurements in DMF/H_2O (1:1, v/v, Tris-HCl buffer，pH=7.4) buffer solution (Fig. S5 and Fig. S6). As shown in Fig. S5, the maximum absorption wavelength was found at 275nm, which attributed to the formation of π-π* transition and polyene π bonds by one triazole ring and more benzene rings[29]. However, the characteristic absorption band of rhodamine B at about 560 nm was not observed, demonstrating its existence in spirolactam form [37]. Fig. S6 is the fluorescence spectra of REDTC measured in the same solution, which showed that the positions of the maximum excitation and emission wavelengths were at 262 nm and 354 nm respectively. Compared to the fluorescence spectroscopy of EDTC(inset in Fig. 1B), it seems that REDTC is a higher polar molecule with the shift of the maximum fluorescence emission peak towards to shorter wavelength from 281 nm to 262 nm [30].

3.3 Spectral characteristics of REDTC for metal cations

It is reported that rhodamine spironolactone or spirolactam compounds are colorless and nonfluorescent, while the corresponding spironolactone/lactam with ring-opening can generate distinct fluorescence emission and show a pink color. In general, a suitable ligand on a spirolactam ring can bring about a color variation along with a fluorescence change in the presence of some metal ions[38]. To get an insight into the binding properties of REDTC toward diverse metal cations, the fluorescence spectra of REDTC (10μM) in DMF-H_2O buffered (20 mM, pH 7.40, 1/1, v/v) solution

upon addition of a wide range of metal cations including Al^{3+}, Pb^{2+}, Mg^{2+}, Mn^{2+}, Hg^{2+}, Fe^{3+}, Zn^{2+}, Mo^{2+}, Cd^{2+}, Cu^{2+}, Na^{+}, Ni^{2+}, Co^{2+} , Ca^{2+} , $K^{+}$and Ag^{+} at the excitation 562 nm were recorded(Fig. 2A). In Fig. 2A, it showed that there was no obvious characteristic emission observed for free REDTC. By comparison to various metal ions, only Hg^{2+} can induce a significant fluorescence enhancement observed at 577 nm accompanied with a color change from colorless to pink, while Ag^{+} could simultaneously cause a very weak fluorescence enhancement.

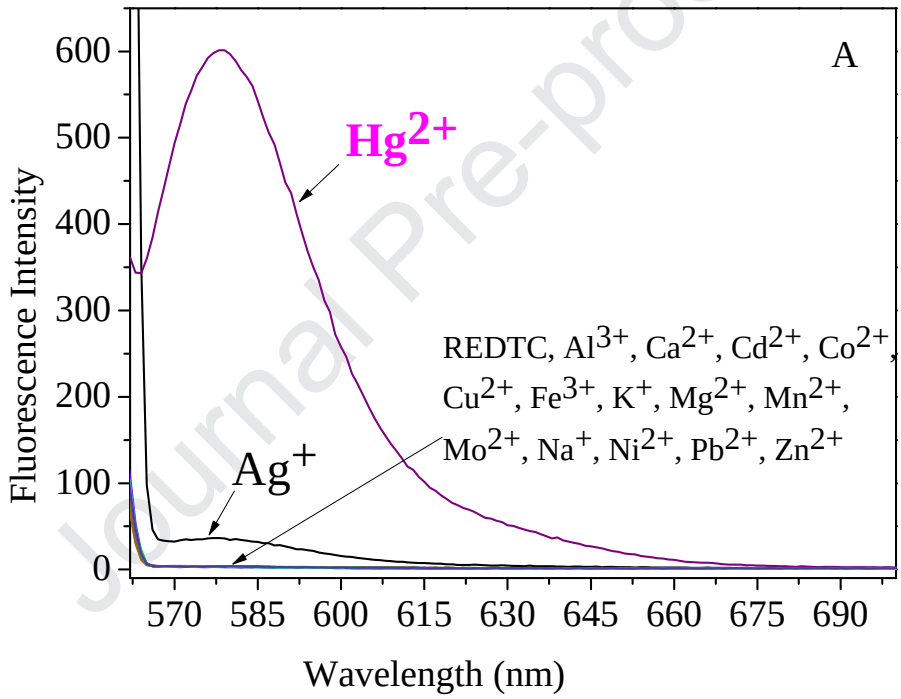

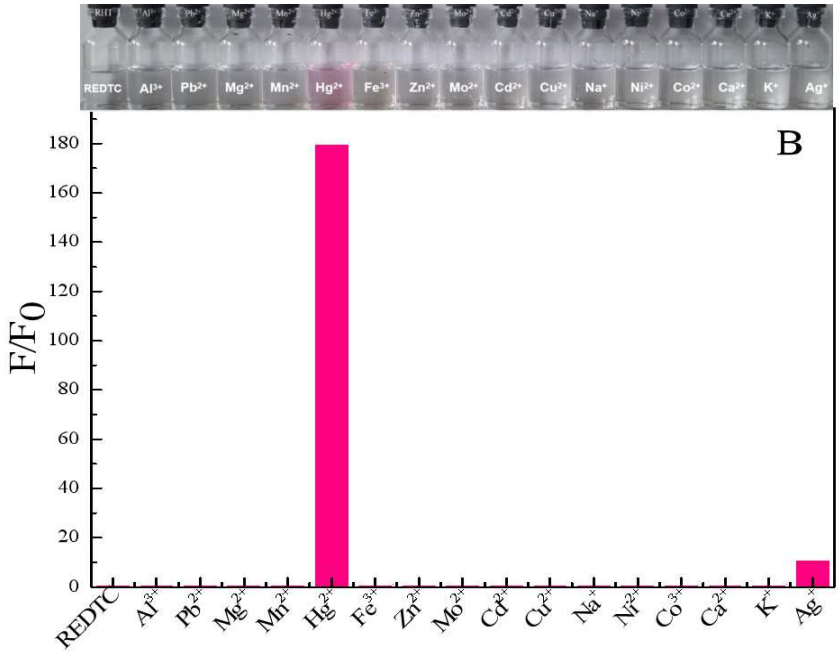

Fig. 2. (A) Fluorescence spectra (a) and fluorescence intensities (b) at 577nm of REDTC (1×10^{-5} mol L^{-1}) in DMF-water (v/v=1/1, Tris-HCl, pH 7.4) in the presence of various cations (5×10^{-5} mol L^{-1}) (λex=562 nm).
(B) Relative fluorescence intensity of the REDTC in the presence of Hg^{2+} and other metal ions. Inset: Photographs of the REDTC in the presence of Hg^{2+} and other metal ions.

The addition of Hg^{2+} to REDTC resulted in a 180-fold increase in fluorescence intensity at 577 nm (Fig. 2B). The inset in Fig. 2B showed photographs of the REDTC in the presence of Hg^{2+} and other metal ions. Other metal ions, such as Al^{3+}, Pb^{2+}, Mg^{2+}, Mn^{2+}, Hg^{2+}, Fe^{3+}, Zn^{2+}, Mo^{2+}, Cd^{2+}, Cu^{2+}, Na^{+}, Ni^{2+}, Co^{2+}, K^{+} and Ca^{2+}ions, did not show any significant color and spectral variation under same conditions except for Ag^{+}, suggesting that Ag^{+} has a slight capacity to induce the spirolactam ring-opening of REDTC to some extent. However, it seems that REDTC possibly generated a new compound with Hg^{2+} and led to a ring opening from the spirolactam (nonfluorescent) to ring-opened amide (fluorescent). The result indicated that REDTC is a more sensitive response to Hg^{2+} ion than other metal ions.

To further detect sensibility of REDTC on Hg^{2+} ions, the fluorescence titration

experiments were carried out upon the gradual addition of Hg^{2+} ions (Fig. 3A). As the increasing concentration of Hg^{2+} ions, it was observed a significant enhancement in the fluorescence intensity of REDTC at 584 nm. However, with the addition of the increasing amount of Hg^{2+} ions, the fluorescence intensity of REDTC gradually became saturated when the concentration of Hg^{2+} reached 46.7μM. The linear fluorescence intensity *vs* the concentration of Hg^{2+} was obtained in the range of 2.80×10^{-5}-4.67×10^{-5}mol /L(R^2=0.9840, Fig. S7). Moreover, the limit of detection of REDTC (1×10^{-5} mol/L) was determined to be 1.61 $\times10^{-9}$ mol/L (3σ/K). The detection limit is equal to 3σ/K, where σ is the standard deviation of the blank solution, K is the slope of the curve of the fluorescence intensity versus the sample concentration [39]. However, a continuous decrease in the fluorescence intensity was observed for further increments of Hg^{2+} concentration. As a result, it seems that RMPTC is special probe in qualitative detection on Hg^{2+} under physiological conditions rather than an ideal probe in the quantitative determination of Hg^{2+}.

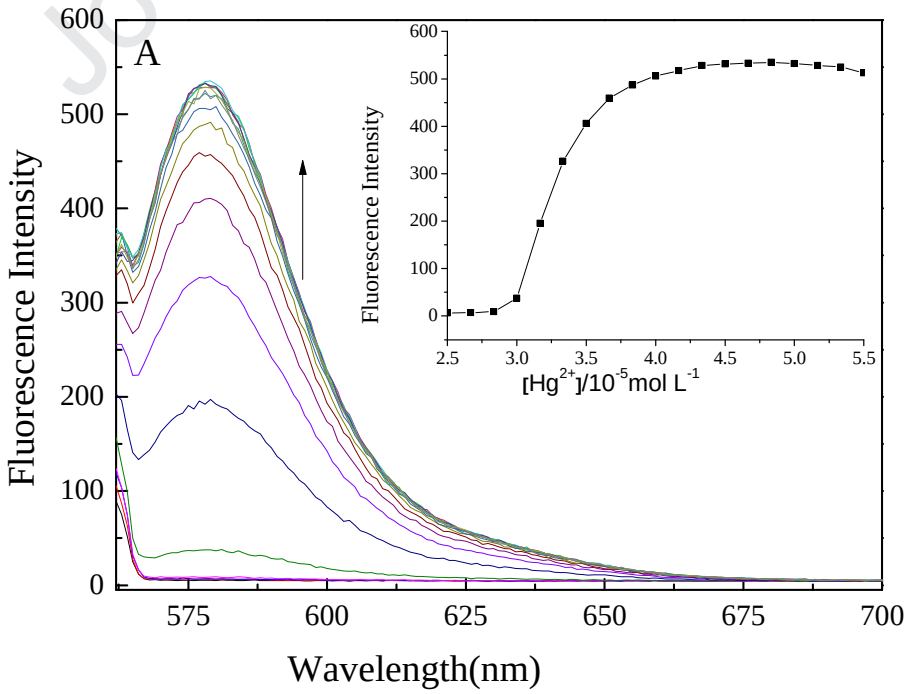

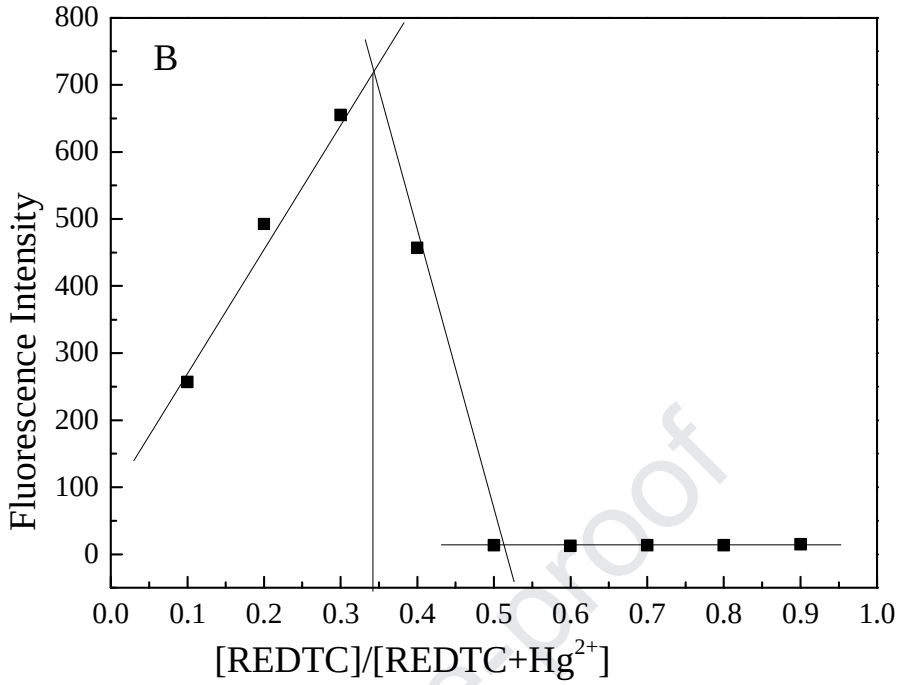

Fig. 3 (A) Fluorescence spectra (λ_{ex}=562 nm) of REDTC (1×10-5 mol /L) upon the addition of Hg^{2+} in DMF-water (v/v=1/1, Tris-HCl, pH 7.40). The illustrationis: graph of the fluorescence intensity at 577 nm as a function of Hg^{2+} concentration.

(B) The Job's plot according to the method for continuous variations, indicating the stoichiometry for REDTC-Hg^{2+} (the total concentration of REDTC and Hg^{2+} is 50μM).

In order to obtain the coordination number of REDTC to Hg^{2+} ions, the job's plot was performed by using the equimolar continuous variations method[40], and the corresponding results were shown in Fig. 3B. It can be seen that the fluorescence intensity at 577nm of the REDTC-Hg^{2+} complex was achieved at a approximate mole ratio of 66.7% of Hg^{2+} ions, which means that a ratio of 1: 2 stoichiometry was the probable binding mode of complex REDTC with Hg^{2+} ions (Fig. 3B) and it confirmed by TD DFT calculations later in this article on proposed mechanism.

The UV-vis spectra of REDTC (50μM) in DMF-H_2O (v/v, 1/1, pH 7.40) buffer solution was measured with the addition of different metal ions (Fig. S8). In Fig. S8,

comparing to the fluorescence spectra, it showed similar results, and the free REDTC also exhibited no absorption near 563 nm. However, it is noted that there is an obvious absorption band appeared at 563 nm in the presence of Hg^{2+}, which was ascribed to the ring-opened rhodamine moieties. Fig. S9 exhibited the spectral change of REDTC upon the increasing Hg^{2+} ions by the UV-vis titration measurements. It can be seen that the absorption strength of REDTC-Hg^{2+} ions system is gradually increased at the position of 563 nm with the increasing Hg^{2+} ions concentration from 2.00×10^{-5} to 4.33×10^{-5} mol/ L. However, with the continuous addition of Hg^{2+} ions, the emergence of platform (inset in Fig. S9) suggested saturation in the reaction between REDTC and Hg^{2+} ions.

3.4 The competition experiments, the effect of pH and reaction time

To evaluate the selectivity of REDTC for Hg^{2+}, the competition experiments under the same conditions were examined in the presence of other metal cations including Al^{3+}, Pb^{2+}, Mg^{2+}, Mn^{2+}, Hg^{2+}, Fe^{3+}, Zn^{2+}, Mo^{2+}, Cd^{2+}, Cu^{2+}, Na^{+}, Ni^{2+}, Co^{2+}, K^{+} and Ca^{2+}ions (Fig. S10). It can be seen that the increasing fluorescence intensity resulting from the addition of Hg^{2+} ions did not change much in the coexistence of other metal ions at the same concentration. The results showed that the presence of cations does not remarkably interfere with the detection of Hg^{2+}; thus, REDTC could be used as a highly selective Hg^{2+} fluorescent probe.

In order to further study the influence of the different acid-base concentration on the spectra of REDTC and found an appropriate pH span in which REDTC could selectively detect Hg^{2+} efficiently, the acid titration experiments were performed. The effect of pH on the emission intensity was examined at a range from 3.0 to 10.0 with a concentration of REDTC fixed at 1×10^{-5} mol /L and Hg^{2+} at 5×10^{-5} mol/ L, respectively (Fig. S11). It can be seen that REDTC showed evident fluorescence when

the value of pH is less than 4 whereas there was no distinct fluorescence observed for REDTC within the limits of the pH range from 4.0 to 10.0. The result implied that the REDTC compound is at the stable spirocyclic state in the pH range of the value of pH. On the contrary the addition of Hg^{2+} led to the fluorescence enhancement over a comparatively wide pH range (4.0-8.0), which was attributed to the opening of the rhodamine ring. Moreover, the optimal fluorescence response toward Hg^{2+} was obtained at the value of pH as 7.4. Consequently, probe REDTC might be used to detect Hg^{2+} in approximate physiological conditions and the spectral studies were carried out in a DMF/H2O solution (1:1, v/v, tris-HCl, pH 7.4).

Besides high sensitivity and selectivity, quick response time is another necessary factor for the detection in real-time. In order to study the response time of REDTC to Hg^{2+}, the changes of the fluorescence intensity at 577 nm on the binding process of Hg^{2+} ion to REDTC was recorded (shown in Fig. S12). It can be seen that the fluorescence intensity of REDTC reached a stable value in less than 3 min and keeps almost unchanged within 12h. So the appropriate response time is 3 min, which can be applied to do the corresponding spectroscopic measurements.

3.5 Proposed mechanism of REDTC response to Hg^{2+}

Combining the above results, a plausible binding mode of REDTC•Hg^{2+}complex is depicted in Scheme 1. This binding mode is consistent with the fluorescence changes observed as the induced conformational alterations of the triazole groups upon 1:2 complexes, which was supported by the ESI-MS spectra and TD DFT calculations. The peak at m/z 1103.2 in the mass spectrum was assignable to the mass of[[REDTC+2Hg-2H] (Fig. 4A(a)), and it was well matched with theoretical mass spectral simulation (calc. 1103.3) (Fig. 4A(b)).

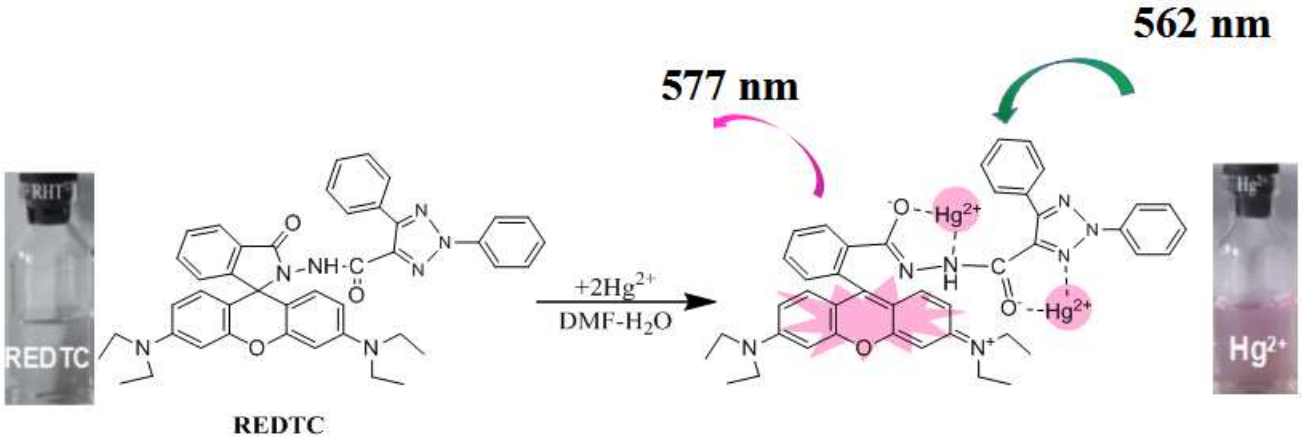

Scheme 1 Proposed recognition mechanism of REDTC towards Hg^{2+}.

To further certify whether the above results are correct or not, the molecular orbitals of REDTC-Hg^{2+} complex was calculated by computational chemistry. The rational structure of REDTC-Hg^{2+} complex was obtained by using the Gaussian 09 program package, and the related results were listed in Table 1 and Fig. 4B. From Fig. 4B, it can be seen that REDTC have two pairs of tongs to bind two Hg^{2+} ions, one of them is the bond by one oxygen atoms and one nitrogen atom from hydrazide group, another one is the bond by another nitrogen atom from triazoles group and another oxygen atoms from carbonyl group. The computer molecular diagram exhibited that REDTC can provide appropriate place to locate two Hg^{2+} ions with two penta cyclic groups generated. The corresponding parameters in Table 1 showed that the values of energy difference of ΔE(a.u.) and ΔE(ev) for REDTC-Hg^{2+}complex as 1:2 stoichiometry were smaller than that of as 1:1 stoichiometry, which indicated that the structure of 1:2 stoichiometry for REDTC binding to Hg^{2+} ions is more stable than that of 1:1 stoichiometries.

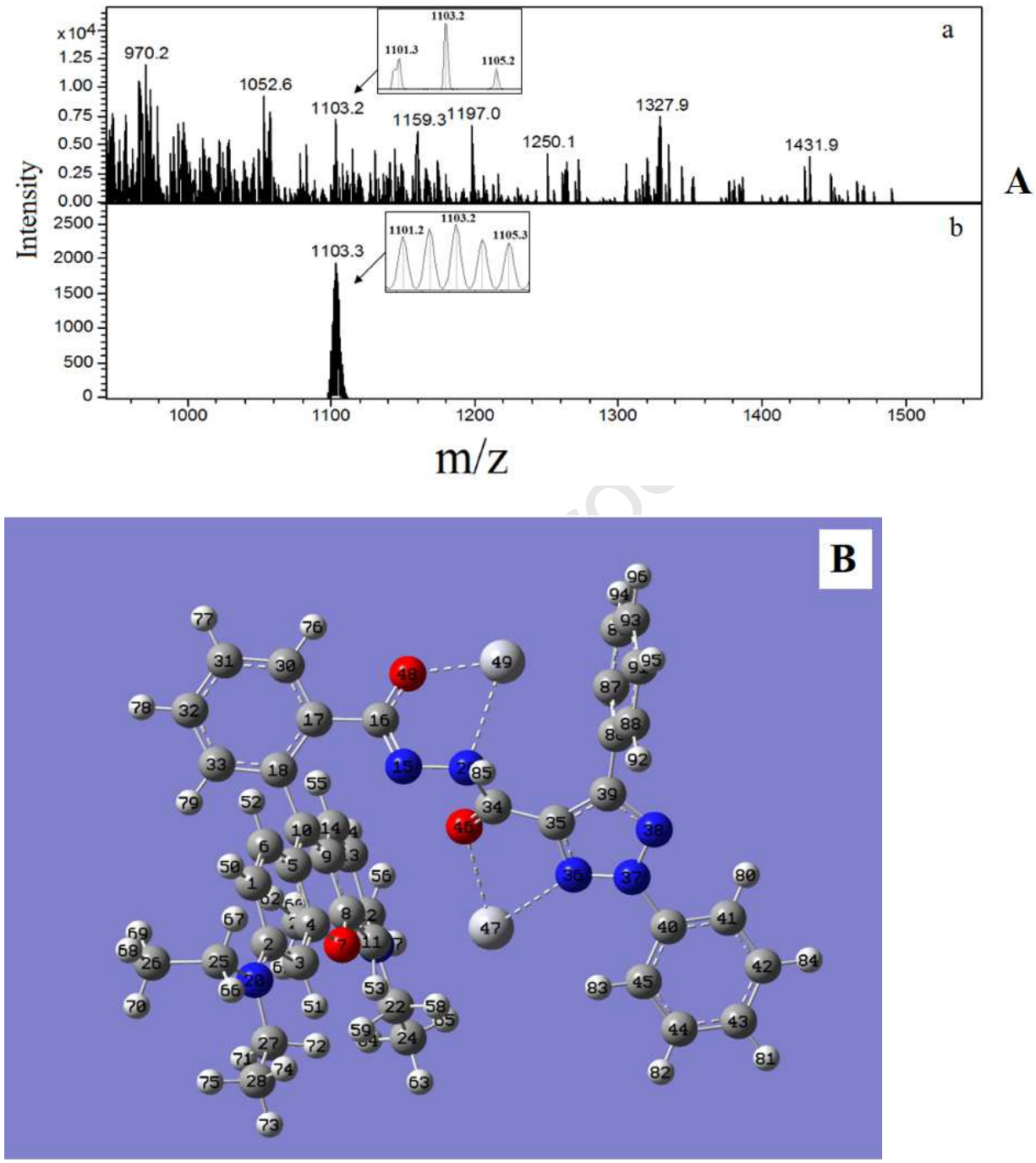

Fig. 4 (A) a: ESI-MS of REDTC in the presence of $Hg^{2+}$and trace amounts of Cl^-.
Inset: enlarged patterns for the [REDTC+2Hg-2H].
b: The calculated ESI-MS of REDTC in the presence of $Hg^{2+}$and Cl^-.
Inset: calculated isotopic patterns for the [REDTC+2Hg-2H].
(B) The optimized structure of REDTC-Hg^{2+}

Table 1 Comparison on energy changes of REDTC binding to Hg^{2+} using the B3LYP functional in Gaussian 09 .

	E_{L1}(a.u.)	E_{Hg}^{2+}(a.u.)	$E_{EDTC\text{-}Hg}^{2+}$(a.u.)	E(a.u.)	E(eV)
EDTC-Hg	-2272.68	-41.794	-2314.92	-0.44	-12.12
EDTC-2Hg	-2272.68	-83.59	-2356.79	-0.52	-14.22

In principle, in order to design an ideal fluorescence sensor systems (the host) for the detection of various analytes (the guest), it is important to develop specific chemical reactions or host-guest interactions that bring about a variation in the spectral properties of the reaction system. If the characteristic reaction between the host and the guest is based on a reversible and noncovalent chemical reaction, and the interaction can be affected under possible conditions, the indicator has named a chemosensor. On the contrary, the binding mode between the guest and the host is an irreversible chemical reaction; the indicator is acted as a chemodosimeter. For chemodosimeters, it is crucial that there are two or more functional groups. One group is the reaction site where the host interacts to the detection object. Moreover, another one is used to offer a luminescent signal that is based on the interaction to the analytes. Both the interaction between the chemodosimeter and analyte and the change in a detectable signal are irreversible [41-42]. Herein, EDTC unit as the reaction site and rhodamine B unit providing spectroscopic signal form the chemodosimeter for detecting Hg^{2+}. So the binding of REPPC to Hg^{2+} ions could cause the formation of the ring-opened state of REPPC from the spirolactam state. Therefore, REDTC would act as a “naked-eye” chemodosimeter probed toward Hg^{2+}, same as to some studies on rhodamine-based fluorescence sensors for characteristic detection of metal ions [41-43].

3.6 Determination of Hg^{2+} in HeLa cell.

In order to examine the practical properties of REDTC in biological samples, the probe was applied for detecting Hg^{2+} in HeLa cell by fluorescence microscopy. As depicted in Fig. 5, a bright field transmission image of cells with Hg^{2+} and REDTC confirmed that the cells were viable throughout the imaging experiments, implying the probe REDTC can penetrate the cell membrane and image Hg^{2+}ions in HeLa cells, with the switching-on fluorescent signal.

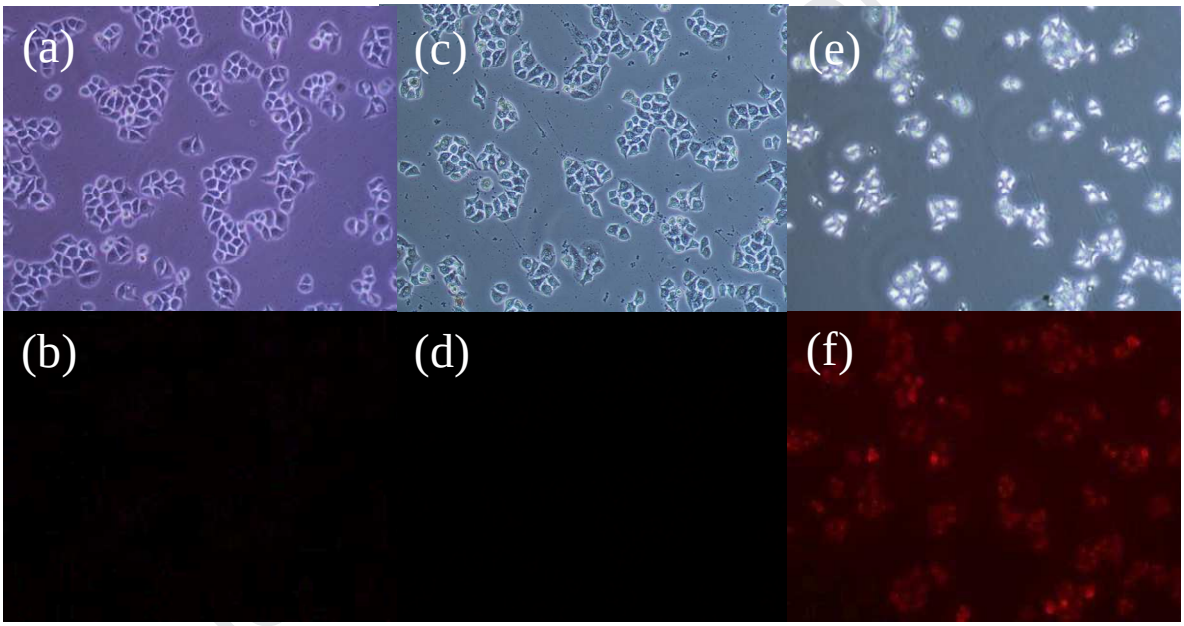

Fig. 5 Fluorescence imaging of Hg^{2+} in HeLa cell with REMPC.
(a, c, and e) Brightfield transmission images;
(b) images of cells incubated with the FBS culture solution as the sample blank;
(d) images of cells incubated with REMPC(10μM);
(f) images of cells incubated with REMPC(10μM) and Hg^{2+} (20μM).

3.7 Compare to other triazoles on detection of Hg^{2+} ions

Based on the above results, there are several similar aspects compared to references on the triazole-based fluorescence probes for detecting Hg^{2+} ions[19, 44-45]. Most of these probes showed excellent selectivity detecting Hg^{2+}

with colour variation from colourless transparent to pink. Moreover, they could enhance the fluorescence signal in methanol or weakly neutral aqueous solution. The stoichiometry of the complex formed between triazoles and Hg^{2+} is 1:1 or 1: 2 ratio in most cases. But there are some differences as well as the following examples. Some triazole-based probes caused diverse change in colour of the solution from colourless transparent to blue-green[46-48], yellow[49-50], or purple[51]. But other probes showed the fluorescence quenching or enhancement without any change in colour[52-53]. Also, there are some differences in the sensitivity and detection limit. The present work indicated that the probe REDTC showed a high selectivity for Hg^{2+} ions but a narrower linear range and a lower sensitivity. However, the advantage of the probe REDTC is that it possessed a high selectivity for sensing Hg^{2+} ions in neutral aqueous solution (pH 7.4) with the triazole appended colorless chemosensor turned to pink and enabled naked-eye detection, which further guides us to explore simple and high-selectivity Hg^{2+} probes in aqueous solutions under physiological conditions.

3.8 The interactions of EDTC binding three blood proteins

The present results illustrated that EDTC could synthesize with rhodamine B to form a novel compound which can be used to detect the chromogenic reaction of Hg^{2+} ion. On the other hand, taking account of the reason that the 1,2,3-triazoles may be further exploited and developed as new drugs, it is necessary to study the interactions with some biological macromolecules. Since the functions of the drugs in the body are the results of their interactions with crucial macromolecules in the organism. Protein is also an essential research object in life science and one of the most vital transport carriers of drugs. Thus, the investigates on small molecular drugs binding targeted

proteins have become more and more important subjects in the field of chemistry, life science and clinical medicine, etc[54].

The selectivity of EDTC (1.67 μM) in tris buffer (pH = 7.4) was evaluated with various amino acids (including Tyr, Lys, Glu, Val, Arg, Met, Cys, Leu, Asn, Pro, Thr, Ala, and Gly, at 1.67 μM) and with three model blood proteins (including HSA, HIg and BHb) (as shown in Fig. S13). From Fig. S13, it can be seen that the distinct decreases were observed after the addition of BHb, while a significant enhancement in fluorescence intensity at 349 nm and 330 nm was created upon the addition of HSA or HIg under identical conditions. However, there was not an obvious variation of fluorescence intensity after the addition of other amino acids. The results make clear that EDTC exhibited excellent selectivity for HSA/HIg/ BHb in tris buffer (pH = 7.4).

Herein, the binding interactions of EDTC with HSA, HIg, and BHb were evaluated by comparing the intrinsic fluorescence intensity of protein before and after the addition of EDTC (Fig. 6A-6C)[55]. These figures showed that the fluorescence intensity of EDTC-protein systems regularly enhanced with increasing concentration of EDTC when excitation wavelength was set at 278 nm. Moreover, the various red shifts of the position of maximum emission wavelength were obtained for all the three proteins, which was 348nm to 356nm for HSA, 331nm to 356nm for HIg and 325nm to 355nm for BHb，respectively. Fig. 6D is the fluorescence emission spectra of EDTC under the same experimental condition as three EDTC-protein systems. It also showed that the fluorescence intensity of EDTC enhanced regularly with increasing concentration of EDTC. It is worth noting that the inset in Fig. 6D can reveal some significant information on the interactions of EDTC and these proteins. Take EDTC-HSA system for example, when the excitation wavelength is set at 278 nm, the value of fluorescence intensity of HSA is 101.76 at 347 nm, the corresponding values

of EDTC is at 365 nm (175.00), and EDTC-HSA is at 355nm (156.15), respectively. It is obvious that there is an interaction between EDTC and HSA, which is similar to EDTC-HIg or EDTC-BHb systems. Therefore, the results suggested that there were strong interactions between the three kinds of proteins and EDTC which were responsible for enhancing the fluorescence of the proteins.

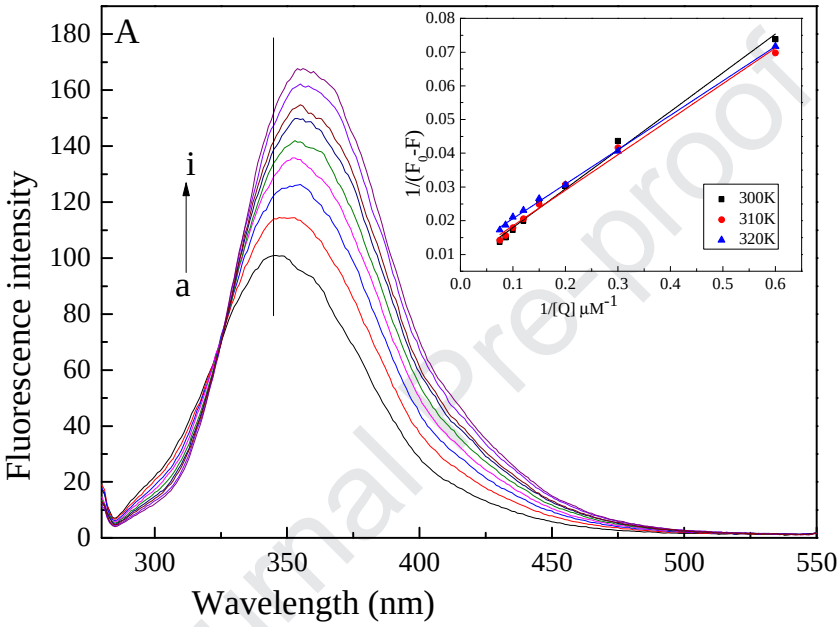

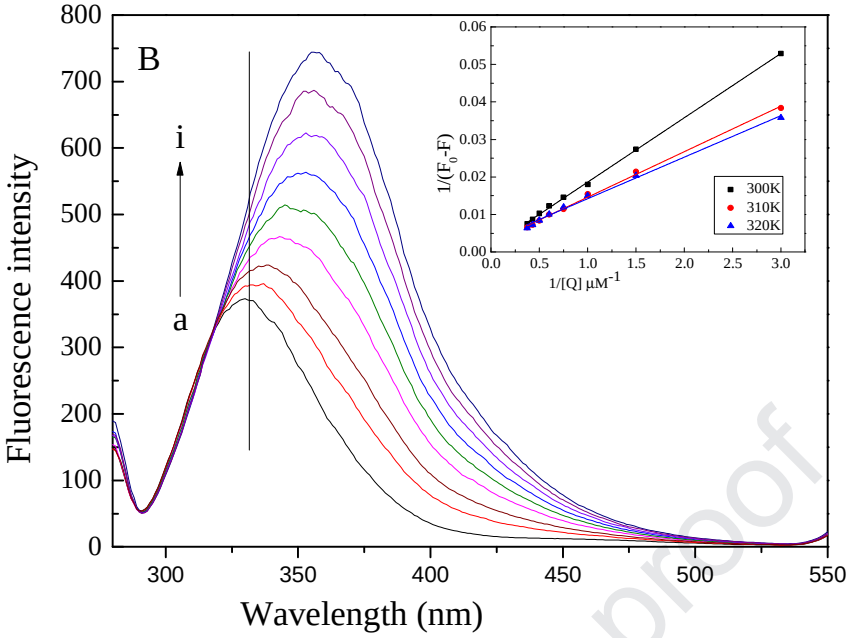

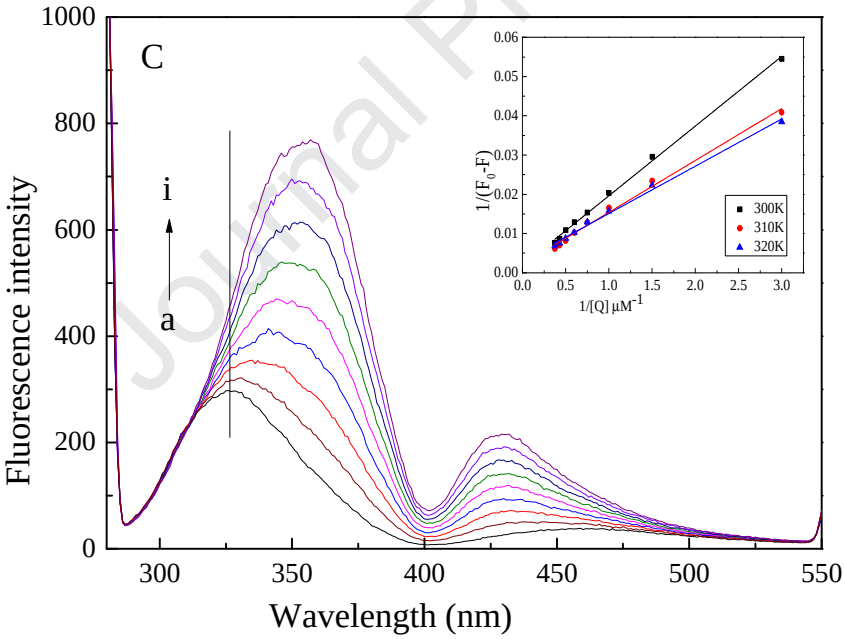

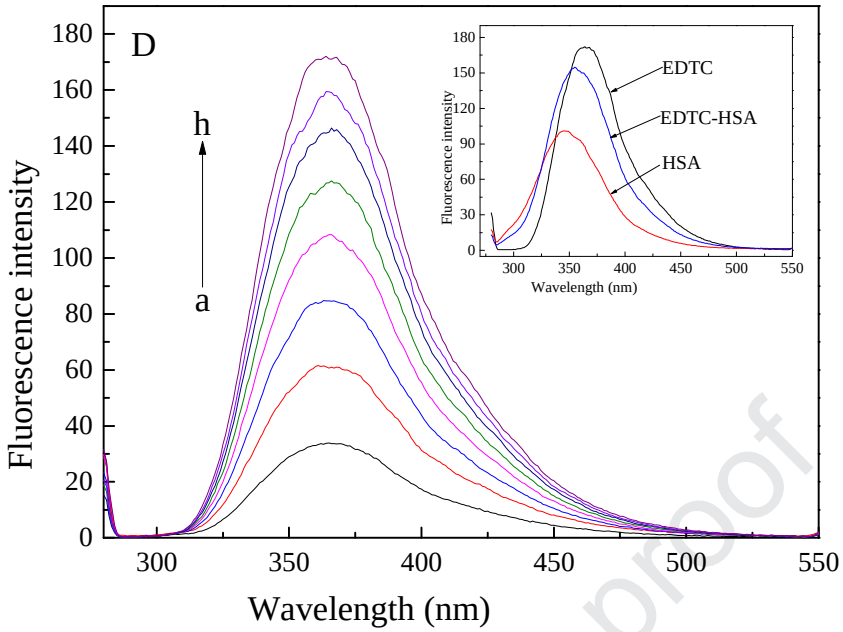

Fig. 6 Fluorescence emission spectra of EDTC-HSA, EDTC-HIgG, EDTC-BHb systems and EDTC in Tris buffer (pH 7.4) at 300 K, λex=278 nm.

(A) EDTC-HSA system, a: HSA (5 μM), b-i: 1.67 , 3.33 , 5 .0, 6.67 ,8.33 , 10.00 , 11.67 and 13.33 μM, respectively.

(B) EDTC-HIgG system, a: HIgG (6×10^{-7}mol /L), b-i: 0.33, 0.67, 1.00, 1.33 , 1.67, 2.00 , 2.33 and 2.67 μM, respectively.

(C) EDTC-BHb system, a: BHb (5μM), b-i: 0.33 , 0.67 , 1.00 , 1.33 ,1.67, 2.00 , 2.33 and 2.67 μM, respectively.

(D) EDTC: 1.67, 3.33, 5.00, 6.67, 8.33, 10.00, 11.67, 13.33μM, respectively.

The illustrations: Plot of $1/(F-F_0)$ against $1/[L]$ for HSA-EDTC system(A), HIgG-EDTC system (B) and BHb-EDTC system (C) at three temperatures (300K, 310K, 320K).

3.9 Binding constants, binding mode, and binding distance

The temperature dependence of the binding constant was measured spectrofluorometrically from the emission spectra of HSA/HIg/BHb in the presence of EDTC in the temperature range of 300K to 320K, and the binding constant value was determined from the fluorescence intensity considering the following equation [56]:

$$1/\Delta F = 1/\Delta F_{max} + (1/K[Q])(1/\Delta F_{max}) \quad (1)$$

Where $\Delta F = F_\chi - F_0$ and $\Delta F_{max} = F_\infty - F_0$, in which F_0, F_χ and F_∞ are the

fluorescence intensities of protein in the absence of EDTC, an intermediate concentration of EDTC, and at the saturation of interaction, respectively; K is the binding constant and [Q], the concentration of EDTC. The linearity of the plot of 1/(F - F_0) against 1/[Q] can determine a binding stoichiometric number by one to one between the two partners (the illustrations in Fig. 6A, 6B and 6C). The binding constants of different EDTC-proteins systems at three temperatures (300, 310 and 320 K) were shown in Table 2 and used to calculate the thermodynamics parameters. From Table 2, it can be seen that the binding constants *K* increased with the increasing temperature for EDTC-HSA, EDTC-HIg, and EDTC-BHb systems respectively. The results indicated that the binding between EDTC and proteins was very strong, and the temperature influenced on it.

According to the classical literature[57], there are primarily four main types of non-covalent interactions existing in the binding of small molecules to biomacromolecules, such as hydrogen bonding, van der Waals forces, hydrophobic and electrostatic interactions. Based on the relevant van't Hoff equations, several thermodynamic parameters including(enthalpy change, ΔH; entropy change, ΔS; and Gibbs free energy change, ΔG) were calculated by the linear relationship between *lnK* and the reciprocal absolute temperature estimated to determine the binding modes and the results were shown in Table 1(plots shown in Fig. S 14). The data from Table 2 indicated that all values of ΔG were negative, which means that the formations of EDTC-HSA , EDTC-HIg and EDTC-BHb complexes were all spontaneous. And the values of ΔH and ΔS were positive, which indicated that the binding processes were endothermic and higher temperature would be advantageous to the formation of EDTC-HSA, EDTC-HIg, and EDTC-BHb complexes. It is reported that the sign and magnitude of the thermodynamic parameters involve various individual kinds of

interaction taking place in protein association processes [57]. In the present work, the positive values of ΔS and ΔH can be greatly owed to the typical hydrophobic interaction, which played the principal role during the binding reactions between EDTC and HSA/HIg/BHb. Moreover, the corresponding value of ΔG attributed more to ΔS than ΔH, meaning the interaction processes were mainly entropy-driven.

Table 2 Binding Parameters and Thermodynamic Parameters for the Binding of EDTC to HSA, HIg or BHb

System	Temperature (K)	*K* ($\times 10^4 M^{-1}$)	r (nm)	ΔG (kJ/mol)	ΔS (J/mol/K)	ΔH (kJ/mol)
EDTC-HSA	300	5.808	5.90	-27.297	174.439	25.032
	310	7.599		-29.041		
	320	10.779		-30.785		
EDTC-HIgG	300	9.935	5.51	-28.774	248.493	45.774
	310	20.440		-31.295		
	320	30.659		-33.744		
EDTC-BHb	300	11.413	3.48	-28.994	204.681	32.411
	310	16.324		-31.040		
	320	25.716		-33.087		

Also the average distances between the EDTC (acceptor) and the protein residues (donor) can be obtained from the Förster theory of dipole-dipole energy transfer theory (FRET)[58]. Since the efficiency of energy transfer (E) is related to the critical distance R_0 and the average binding distance (r) between the acceptor and donor. The basic condition to determine the binding distance is that there is an overlap of the absorption spectrum of EDTC and the fluorescence emission spectrum of proteins. In Fig. S15, the overlaps of the absorption spectrum of EDTC and the emission spectrum of HSA/HIg/BHb were illustrated, and the related equations were applied to calculate the values of r and R_0[58]. Thereinto several rational parameters could be selected as $\kappa = 2/3$, $\Phi_d = 0.118$, $\eta = 1.36$ according to the literature[59], and

the results were listed in Table 1. It can be seen that the binding distances r between EDTC and the amino acid residue in HSA, HIg or BHg, were found to be 5.90 nm, 5.51 nm, and 3.48 nm, respectively. It was apparent that the EDTC-proteins distances are less than 7 nm, which implies that the energy transfer from HSA/HIg/BHb to EDTC occurred with a high possibility.

3.10 Binding-induced conformational changes of proteins

Recently lots of research indicated that protein conformational changes were bound up with specific properties including assembly, function, transportation, potential cytotoxicity, and tendency to aggregate[60-61]. The possible influence of binding of EDTC to HSA, HIg, or BHg on the secondary structure of the three blood proteins was investigated by UV-visible, synchronous fluorescence, and 3D fluorescence spectroscopy.

The information from near-UV absorption spectra of aromatic amino acid residues in proteins usually involved in protein conformations. The maximum absorbing peak at about 210 nm can represent the framework conformation of the protein, and that of at about 280 nm can reflect the information on tryptophans(Trp), tyrosine(Tyr) and phenylalanine(Phe) residues[62]. The spectral peaks in the range between 250-265 nm correspond to Phe residues, and those in the region 265-280 nm attribute to the electronic interactions of Trp and Tyr residues, whereas the spectral peaks above 285 nm are considered exclusively as Trp residues contributions[63]. Fig. 7 is the UV-vis absorption spectra of EDTC(Fig. 7A), and HSA/HIg/BHb with different concentrations of EDTC(Fig. 7B-7D) as can be seen in Fig. 7A, the chromophore of EDTC gives a characteristic dual absorbance spectrum at 209 nm and 280 nm, which is different from the result of Fig. 2(A) and indicated an obvious solvent effect. In Fig. 7B-7D, the similarity is that free HSA /HIg/BHb has

strong absorbance with a peak at round 211 nm and the absorbance of three proteins increased with the addition of EDTC. However, there is some difference between their shoulder peaks. It showed that the positions of maximum absorbance wavelength are slightly shifted from 272 nm to 277 nm for EDTC-HSA system, 274 nm to 281 nm for EDTC-HIg system and 270 nm to 276 nm for EDTC-BHb system, respectively. Above all, there is another peak occurred at 402nm for EDTC-BHb system, which displayed the special spectral characteristic of BHb. As a result, EDTC can bind three proteins due to Trp and Tyr electronic interactions and generated the conformational changes in HSA/HIg/BHb.

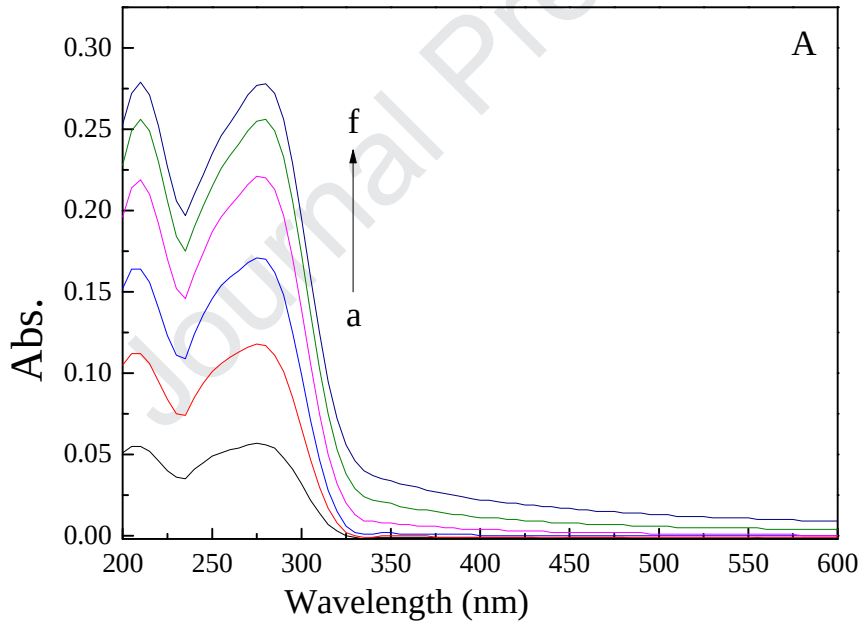

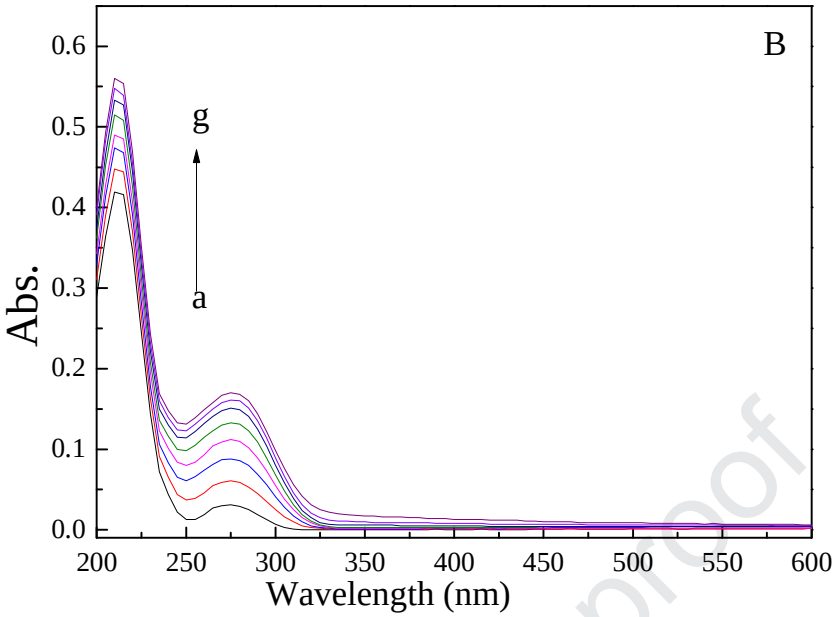

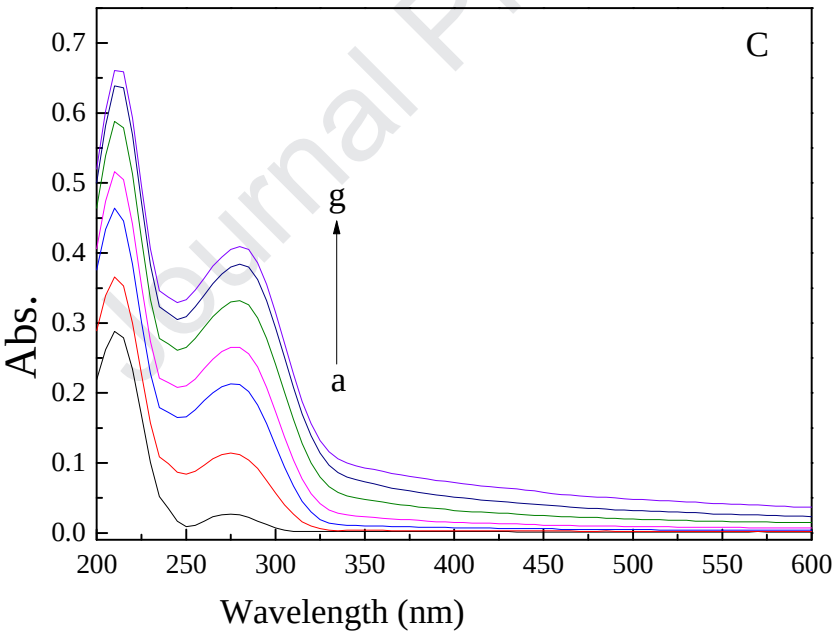

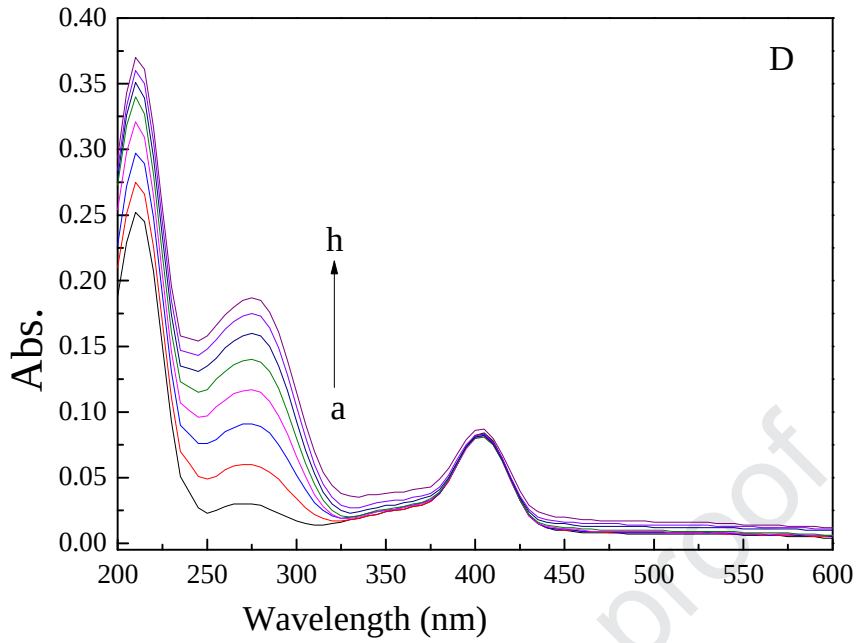

Fig. 7 UV-vis absorption spectra of EDTC, EDTC-HSA, EDTC-HIgG, EDTC-BHb systems and EDTC in Tris buffer (pH 7.4) at 300 K.
(A) EDTC: 1.67, 3.33, 5.00, 6.67, 8.33, 10.00, 11.67, 13.33μM, respectively.
(B) EDTC-HSA system, a: HSA (5 μM), b-i: 1.67, 3.33, 5.0, 6.67,8.33, 10.00, 11.67 and 13.33 μM, respectively.
(C) EDTC-HIgG system, a: HIgG (6×10^{-7}mol /L), b-i: 0.33, 0.67, 1.00, 1.33, 1.67, 2.00 , 2.33 and 2.67 μM, respectively.
(D) EDTC-BHb system, a: BHb (5μM), b-i: 0.33 , 0.67 , 1.00 , 1.33 ,1.67, 2.00 , 2.33 and 2.67 μM, respectively.

The synchronous fluorescence spectra is another common approach providing information on the molecular environment of protein in the vicinity of the chromophore molecules by measuring the possible shift in the position of maximum emission wavelength. The properties of Try residues or Trp residues can be charactered by the synchronous fluorescence of protein when the value of $\Delta\lambda$ is set at 15 nm or 60 nm, respectively[64]. It is reported that Trp resides probably situated at the nonpolar location and embedded in a hydrophobic cavity in protein if the maximum emission wavelength (λ_{max}) is in the range of 330 to 332nm; while Trp residues are exposed to water when λ_{max} is set between 350 to 352 nm, which means

that λ_{max} in 350-352 nm shows that Trp residues are exposed to water, the hydrophobic pocket in proteins is unconsolidated, and the structure of protein is looser [65]. The figures in Fig. S16 is the synchronous fluorescence spectra of three EDTC-proteins systems at the wavelength interval ($\Delta\lambda$ = 60 nm) and the corresponding illustrations ($\Delta\lambda$ =15 nm). With continuous addition of EDTC concentrations, it is found that the fluorescence intensity of three EDTC-proteins systems enhanced and the position of maximum emission wavelength was shifted from 340 nm to 345 nm for EDTC-HSA system, 333 nm to 341 nm for EDTC-HIg system and 334 nm to 345 nm for EDTC-BHb system, respectively. These suggested that the microenvironments around three proteins were changed in the presence of EDTC and EDTC can lead to the exposure of Trp residues of three proteins embedded in nonpolar hydrophobic cavities were moved to a more hydrophilic surroundings. The insets in Fig. **S**16 showed that there have no significant shift in the position of fluorescence emission peak wavelength but slight decreases of emission intensity at about 301 nm in some way. It is worth noting that there is a concomitant increase in the fluorescence emission at 309 nm in the illustration of Fig. S16 (A), which is the characteristic wavelength of the bound-HSA. This phenomenon might be the result of the radiationless energy transfer between EDTC and HSA, which has been confirmed by Förster resonance energy transfer theory. These observations explained that the microenvironment around Tyr residues of HSA/HIg/BHb had little change. Moreover, the various extent on the red shift of λ_{max} for Trp residues larger than that of Tyr residues suggested that the binding location of EDTC is near to the Trp moiety of proteins. All in all, these results illustrated that EDTC is mainly bound to the hydrophobic cavity of HSA/HIg/BHb, which is by the following results of molecular modeling.

Moreover, the information from three-dimensional(3D) fluorescence spectroscopy can reveal some structural and conformational properties of proteins when the excitation and emission wavelengths were simultaneously changed. The position of the maximum emission wavelength and the fluorescence intensity of the amino acid residues have a close connection with the polarity of their microenvironment [66-67]. The figures in Fig. S17 showed the 3D fluorescence spectra and contour spectrum for EDTC-protein systems in the presence and absence of EDTC and the related characteristic parameters are listed in Table S2. In these six spectra, each peak named “peak a” is the first order Rayleigh scattering peak($\lambda_{ex} = \lambda_{em}$) and those “peak b” is the second order scattering peak($2\lambda_{ex} = \lambda_{em}$), respectively [68]. Each peak “1” around 280 nm chiefly exhibits the spectral characteristic of Trp and Tyr residues and that of peak “2” around 230 nm discloses the information on the fluorescence spectral behavior of polypeptide backbone structures, which can be due to the transition of π-π* of protein's special polypeptide backbone structure C=O [69]. Therefore, these figures indicated that not only there are similar increasing trends on the fluorescence intensity of the main characteristic peaks for proteins in the presence of EDTC but also the position of these peaks shifted to different wavelength in some degree, which further demonstrated that EDTC interacted with three blood proteins. Moreover, the enhancement of the fluorescence emission intensity of these peaks named “peak 2” showed that EDTC had impacts on the macromolecular peptide backbone structures of three proteins. The peaks called “peak 1” also reflected the changes in the microenvironment of Trp and Tyr residues, and moreover, EDTC brought about conformational variation in the secondary structure of HSA/HIg/BHb. Simultaneously, a red shift could be found in the maximum emission wavelength for each peak 1, and the related values of the Stokes shift were list in Table 3. All in all,

the above results suggested that the binding of EDTC to three proteins caused a slight unfolding of the polypeptide chain of three proteins.

3.11 Molecular docking analysis

Molecular docking technique can be used to visually display plausible protein-ligand interactions and further provide evidence supporting the experimental result. Herein, the AutoDock program is carried out to ascertain the binding mode of EDTC on HSA, HIg, or BHb. The 3D docked models of EDTC to three proteins are shown in Fig. 8, in which the zonal and stick binding pattern between EDTC and the proteins and only residues around 8 Å of EDTC are displayed.

An earlier report on the structural property of HSA showed this heart-shaped protein is a single-chain, non-glycosylated polypeptide that includes 585 amino acids with an approximate molecular weight of 6,500 Da. There are three homologous domains I-III with the dimension of 80 × 80 × 30 Å, each of which possesses two sub-domains A and B that are composed of 4 and 6-helices under physiological conditions [70]. According to the rational Sudlow's classification, small molecular drugs are usually located in two main binding sites called subdomain IIA and IIIA(sites I and site II respectively) [71]. The two sites are primarily helical and universally cross-linked based on some disulfide bridges with a tryptophan residue (Trp214) in site I [72]. Another well-known literature revealed that subdomain IB (site IB) maybe the third major drug-binding location of HSA[73]. Fig. 8A is the best-scoring binding modes associated with affinity -5.013 kcal /mol between the HSA and EDTC with the labeled chief residues. The molecular simulation with maps of EDTC binding to HSA manifested that EDTC was surrounded by Leu-491, Phe-488, Ser-489, Leu-453, Tyr-411, Arg-485, Val-426, Ala-449, Arg-410, Leu-430, Leu-387, Ile-388, Phe-403 and Asn-391, illustrating the existence of hydrophobic

interaction between EDTC and HSA. Simultaneously, there is a hydrogen bond observed between nitrogen and the hydrogen of hydroxyl of Tyr-411, which indicated that the existence of hydrogen bond reduced the hydrophilicity and enhanced the hydrophobicity to stabilize the EDTC-HSA system [74]. In view of spectral quality of proteins, Tyr, Trp, and Phe residues are commonly intrinsic chromophores and are answerable for fluorescence [63]. Then obviously, the moiety of EDTC is in very close proximity to Tyr 411, Phe 403 and Phe 489 residues of HSA, which further provides a structural information on the fluorescence energy transfer of these residues to EDTC and the efficient fluorescence enhancement of HSA emission in the presence of EDTC.

Another used model protein, human immunoglobulin G (IgG), is part of the family of five classes of antibodies, which mediates a characteristic biological response following antigen interaction. The reported crystal structure has exhibited that IgG contains two the same heavy chains including about 450 amino acid residues and two identical light chains including about 210-230 amino acid residues, which seems like a “T” or “Y” shaped molecule with three compact spheres connected through a hinge region. A complex of the N-terminal regions including the two L and H chains can form both of antigen-binding sites of the IgG molecules, which are combined by links to the C-terminal carbohydrate tail (Fc fragment) generated from the H chains alone and show higher specificity and affinity to many drugs[75-76]. Fig. 8B is the best-scoring binding modes associated with affinity -3.648 kcal /mol between the HIg and EDTC with the labeled pivotal residues. It showed that there is one hydrogen bond between the H atoms of EDTC with Thr 67 of HIg. Moreover, the two aromatic rings of EDTC and one triazole ring illustrate hydrophobic interactions to hydrophobic parts of Pro-95, Trp-23 and Val-94, respectively. Similarly, EDTC is

in very close proximity to Trp residue of HIg, which also as sound evidence to state the efficient fluorescence enhancement of HIg in the presence of EDTC.

Bovine hemoglobin (BHb), as the main blood protein, is a foremost important representative of hemoprotein and here performed to study the binding to EDTC. The crystalline structure of hemoglobin consists of four heme prosthetic groups and four polypeptide chains, where the iron atoms are present in the ferrous (Fe^{2+}) state. The globin or protein fraction contained two α-chains and two β-chains, in which the α-chains contain seven and the β-chains contain eight helical regions, respectively. Each chain is answerable for locating one heme group in a pocket, in which oxygen and other ligands can bind reversibly [77-78]. Fig. 8C displayed the best-ranked result, which has the lowest free energy for EDTC-BHb system associated with affinity -5.099 kcal /mol between the BHb and EDTC with the labeled prime residues. It can be seen that the binding site was mainly composed with 12 amino acid residues including Leu-29, Val-62, Lys-61, Phe-46, Ala-65, His-58, Leu-83, Phe-43, His-45, His-87, Leu-91, and Leu-86, respectively. These results indicated that hydrophobic interaction occurred between EDTC and BHb. Moreover there was three hydrogen bonding interaction between EDTC, and the protein backbone, one of them is between the nitrogen of EDTC and the hydrogen of His-58, another one is between the oxygen of EDTC and the hydrogen of His-58, and the third is between the oxygen of EDTC and hydrogen of amino of Lys-61. So these hydrogen bonds combining hydrophobic interactions play a vital role in stabilizing EDTC-BHb system. Simultaneously, it is noted that Phe 43 and Phe 46 residues of BHb are very near to the constitutional unit of EDTC, which may cause the fluorescence emission enhancement of the protein.

The above results on molecular simulations confirmed that the ligand binding regions of HSA/HIg/BHb were mainly located in hydrophobic cavities, in which are

sufficient to contain the structure of EDTC in the binding pockets of the three proteins. These studies of computational molecular modeling are in good agreement with the spectral experimental results.

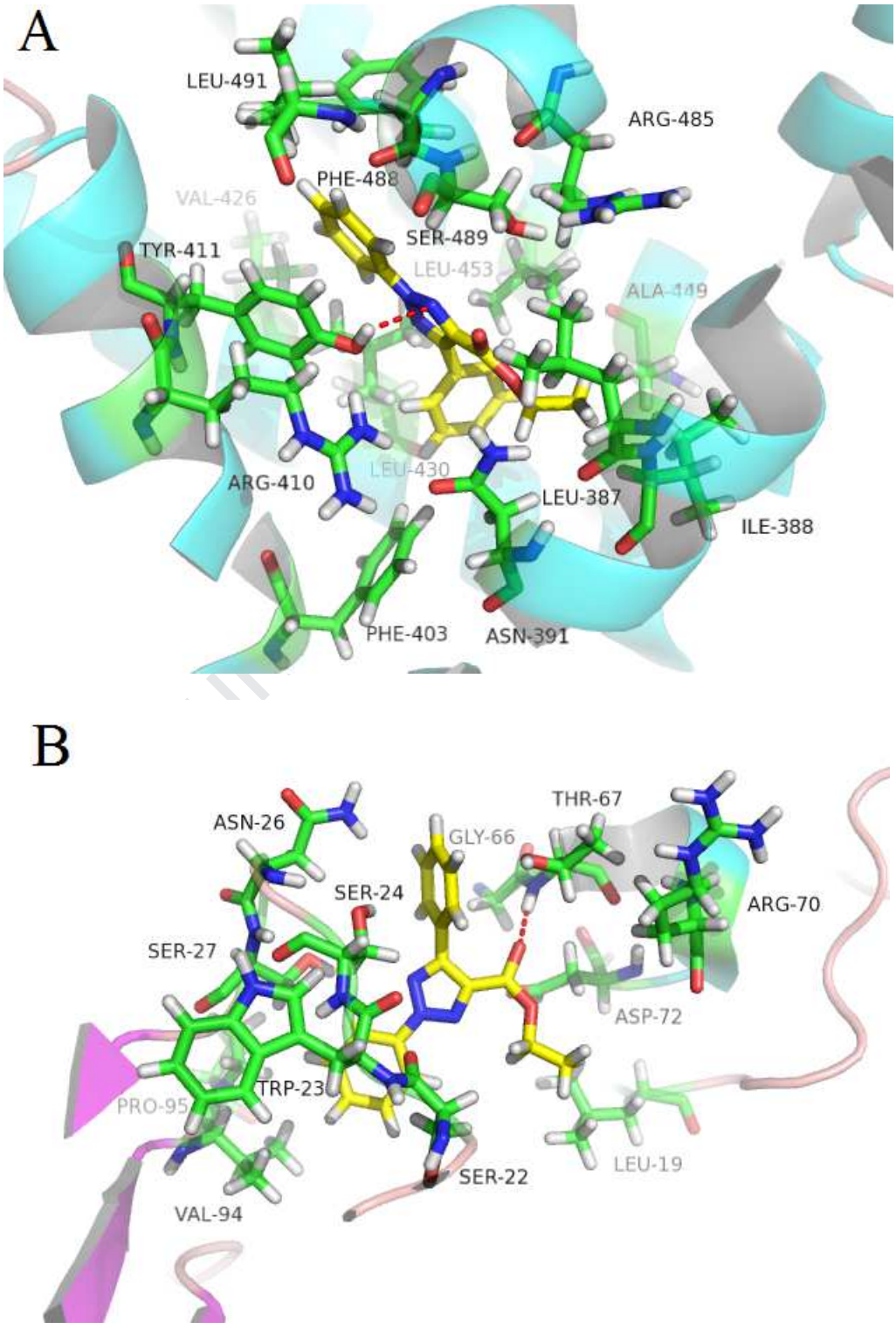

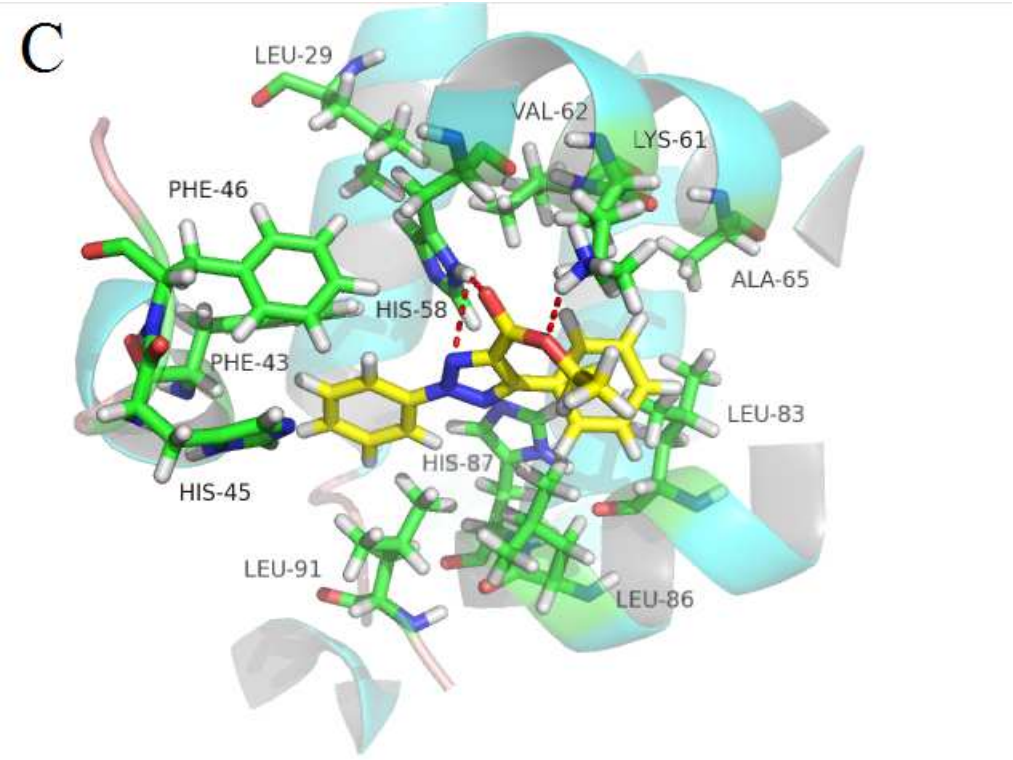

Fig. 8 The binding mode between EDTC and HSA(A), HigG(B) and BHb(C). Only residues around 8 Å of EDTC were displayed. The residues of HSA/HIgG/ BHb and the EDTC structure were represented using ball and stick model. The hydrogen bond between EDTC and HSA/HIgG/BHb is represented using dashed line.

3.12 Compare to other triazoles on binding with various proteins

The aim of present work is to study the specific binding of a new 1,2,3-triazole to three blood proteins and reveal the binding effectiveness of EDTC as drugs.

Also, the above achievements indicated that the triazole EDTC could strongly bind to three typical blood proteins, which implied that EDTC has good stability for controlled drug delivery and a satisfactory prospect in the release drug delivery system. Compare to EDTC, other triazoles have also been widely studied for their broad range of binding activity to different proteins. Tummala et al. found certain 3,4,5-trisubstituted 4H-1,2,4-triazoles as moderately potent inhibitors of the interaction between annexin A2 and the S100A10 protein[79]. It is reported that there was the competitive interactions between a novel berberine

triazole and metal ions to HSA[80]. Gao et al. discovered that triazole density of a resin played the crucial role in determining the extent of non-specific protein adsorption[81]. Lv et al. synthesized and explored as antimicrobial agents a series of some new 1,2,3-triazole-derived naphthalimides. The experimental results indicated the blood protein HSA could effectively store and carry compound 9e by electrostatic interaction[82]. A recent research studied by Chen et al. has showed fragment-based drug discovery of triazole inhibitors to block PDEδ-RAS protein-protein interaction[83].

4. Conclusions

In summary, a new chemosensor (REDTC) with 1, 2, 3-triazole as subunit (EDTC) has been designed and synthesized. The probe showed high selectivity to Hg^{2+} ions by using the fluorescence and UV-vis absorbance spectroscopy along with a pink chromogenic reaction. The triazole appended rhodamine chemosensor REDTC displayed selective complexation with Hg^{2+} even in the presence of other competitive metal ions. The 1:2 stoichiometry of the complex formed between chemosensor REDTC and Hg^{2+} showed the potential for the quantitative determination of Hg^{2+} ions. Fluorescence imaging of Hg^{2+} in HeLa cells was successfully operated, demonstrating that REDTC is of favorable membrane-permeable property for the biological imaging applications. Also, the binding mechanisms of EDTC to three blood proteins (HSA, HIg, and BHb) were determined through UV-vis, fluorescence spectroscopy, and molecular docking under simulated physiological conditions. Exceptional fluorescence enhancements of three blood proteins occurred during EDTC binding by non-covalent interactions, which resulted in a differernt variation of the secondary structure of these proteins and were measured by several spectroscopy methods in the presence of EDTC. The thermodynamic parameters confirmed that

hydrophobic interactions played crucial roles in stabilizing these complex, which is correspond with the results from molecular docking. These results demonstrate that the binding of EDTC to HSA/HIg/BHb caused some conformational changes of the biomacromolecules, signifying that EDTC may have a notable effect on the biological activity of blood proteins when used in the biological system. This research was an improvement for the application of 1,2,3-triazole compound and guides for using simple and high-selectivity Hg^{2+} probes in aqueous solutions and utilization in biological activity.

Acknowledgments

This work is financially supported by National Natural Science Foundation of China (No. 21562019); Hainan Provincial Natural Science Foundation of China (No. 219MS040); Hainan province natural science foundation of innovative research team project（2016CXTD007).

Reference

[1] C. W. Tornøe, C. Christensen, M. Meldal, Peptidotriazoles on Solid Phase: [1,2,3]-Triazoles by Regiospecific Copper(I)-Catalyzed 1,3-Dipolar Cycloadditions of Terminal Alkynes to Azi, J Org. Chem. 67 (2002) 3057-3064.

[2] J. Totobenazara, A. J. Burke, New click-chemistry methods for 1, 2, 3-triazoles synthesis: recent advances and applications, Tetrahedron Lett. 56 (2015) 2853-2859.

[3] N. N.E. El-Sayed, M. A. Abdelaziz, W. W. Wardakhan, R. M. Mohareb, The Knoevenagel reaction of cyanoacetylhydrazine with pregnenolone:Synthesis of thiophene, thieno [2, 3-d] pyrimidine, 1, 2, 4-triazole, pyran and pyridine derivatives with anti-inflammatory and anti-ulcer activities, Steroids 107 (2016) 98-111.

[4] R. Gup , O. Erer , N. Dilek,One-pot synthesis of a new 2-substituted 1,2,3-triazole 1-oxide derivative from dipyridyl ketone and isonitrosoacetophenone hydrazone: Nickel(II) complex, DNA binding and cleavage properties, Bioorg. Chem. 71 (2017) 325-334.

[5] G. Aromi, L.A. Barrios, O. Roubeau, P. Gamez, Triazoles and tetrazoles: prime ligands to generate remarkable coordination materials, Coord. Chem. Rev. 255 (2011) 485-546.

[6] A. Maisonial, P. Serafin, M. Traıkia, E. Debiton, V. Thery, D.J. Aitken, P. Lemoine, B. Viossat, A. Gautier, Click chelators for platinum-based anticancer drugs, Eur. J. Inorg. Chem. 2 (2008) 298-305.

[7] H. Yang , Z. G. Zhou , K. W. Huang , M. X. Yu , F. Y. Li , T. Yi , C. H. Huang, Multisignaling Optical-Electrochemical Sensor for Hg^{2+} Based on a Rhodamine Derivative with a Ferrocene Unit. Org. Lett. 9 (2007) 4729-4732.

[8] K. Wechakorna, K. Suksenc, P. Piyachaturawat, P. Kongsaeree, Rhodamine-based fluorescent and colorimetric sensor for zinc and its application in bioimaging, Sensor Actuat. B 228 (2016) 270-277.

[9] Y. S. Jeong, J. Y. Yoon, Recent progress on fluorescent chemosensors for metal ions, Inorg. Chim. Acta 381 (2012) 2-14.

[10] S. Erdemir, S. Malkondu,A simple triazole-based “turn on” fluorescent sensor for Al^{3+} ion in MeCN-H_2O and F^- ion in MeCN, J. Lumin. 158 (2015) 401-406.

[11] Y. W. Wang, L. X. Wang, F. P. An, H. Xu, Z. J. Yin, S. R. Tang, H. Hao Yang, H. B. Song, Graphitic carbon nitride supported platinum nanocomposites for rapid and sensitive colorimetric detection of mercury ions, Anal. Chim. Acta 980 (2017) 72-78.

[12] C. Y. Song, B. Y. Yang, Y. Zhu, Y. J. Yang, L. H. Wang, Ultrasensitive sliver nanorods array SERS sensor for mercury ions, Biosens. Bioelectron. 87 (2017) 59-65.

[13] L. Y. Wu, S. Guo, X. H. Wang, Z. F. Guo, G. G. Yao, Q. Lin, M. S. Wu, Tandem synthesis of 2-aryl-1,2,3-triazoles from α-arylhydrazonoketones with NH4OAc via copper-catalyzed aerobic oxidation, Tetrahedron Lett. 56 (2015) 2145-2148.

[14] R. O. Dror, H. F. Green, C. Valant, D. W. Borhani, J. R. Valcourt, A. C. Pan, D. H. Arlow, M. Canals, J. R. Lane, R. Rahmani, J. B. Baell, P. M. Sexton, A. Christopoulos, D. E. Shaw, Structural basis for modulation of a G-protein-coupled receptor by allosteric drugs, Nature. 503 (2013) 295-299.

[15] W. Y. He, H. M. Shu, Z. D. Hu, The Spectroscopic Studies and its Application on the Interaction between Small Molecule and Protein, Science Press, Beijing , 2012.

[16] T. Peters, All About Albumin:Biochemistry, Genetics,and Medical Applications, Elsevier Science,1995.

[17] S. Zhang, N. Huang, Q. Lu, M. Liu, H. Li, Y. Zhang, S. Yao, A double signal electrochemical human immunoglobulin G immunosensor based on gold nanoparticles-polydopamine functionalized reduced graphene oxide as a sensor platform and AgNPs/carbon nanocomposite as signal probe and catalytic substrate, Biosens. Bioelectron. 77 (2016) 1078-1085.

[18] D. Q Yang, H. J. Meng, Y. F. Tu, J. L. Yan, A nanocluster-based fluorescent sensor for sensitive hemoglobin detection, Talanta 170 (2017) 233-237.

[19] S. Erdemir, O. Kocyigit, S. Malkondu, Detection of Hg^{2+} ion in aqueous media by new fluorometric and colorimetric sensor based on triazole-rhodamineS. J. Photochem. Photobiol. A 309 (2015) 15-21.

[20] N. Cacita, S. Nikolaou,Studying the interaction between trinuclear ruthenium complexes and human serum albumin by means of fluorescence quenching, J. Lumin. 169 (2016) 115-120.

[21]M. I. Halawa, W. Y. Gao, M. Saqib, S. A. Kitte, F. X. Wu, G. B. Xu,Sensitive detection of alkaline phosphatase by switching on gold nanoclusters fluorescence quenched by pyridoxal phosphate, Biosens. Bioelectron. 95 (2017) 8-14.

[22] F. Ge, H. Ye, J. Z. Luo, S. Wang, Y. J. Sun , B. X. Zhao, J. Y. Miao, A new fluorescent and colorimetric chemosensor for Cu(II) based on rhodamine hydrazone and ferrocene unit, Sensor Actuat. B 181 (2013) 215-220.

[23] X. X. Wang, X. L. Li, W. Shi, S. Wei, J. P. Giesy, H. X. Yu, Y. L. Wang. Docking and CoMSIA studies on steroids and non-steroidal chemicals as androgen receptor ligands, Ecotoxicol. Environ. Saf. 89 (2013) 143-149.

[24] Y. C. Chou, The low-lying singlet electronic excited states of ZrO2: A symmetry adapted cluster-configuration interaction (SAC-CI) study, Comput. Theor. Chem. 1069 (2015) 112-118.

[25] N. Anusuya, P. Sounthari, J. Saranya, K. Paramswar, S. Chitra, Quantum Chemical Study on the Corrosion Inhibition Property of Some Heterocyclic Azole Derivatives, Orient. J. Chem. 31 (2015) 1741-1750.

[26] X. H. Li, H. L. Cui, R. Z. Zhang, X. Z. Zhang, Theoretical investigation on the non-linear optical properties, vibrational spectroscopy and frontier molecular orbital of (E)-2-cyano-3-(3-hydroxyphenyl)acrylamide molecule, Spectrochim. Acta, Part A 137 (2015) 321-27

[27] L. Z. Han, Z. Wang, Y. J. Hua, A. M. Ren, Y. L. Liu, P. J. Liu, Optical and electronic properties of tris [4-(9-phenylfluoren-9-yl) phenyl] amine as light-emitting materials, J. Mole. Science 26 (2010) 168-172.

[28] H. A. Kurtz, J. J. P. Stewart, K. M. Dieter, Calculation of the nonlinear optical properties of molecules, J. Computat. Chem. 11 (1990) 82-87.

[29] M. H. Zhu, P. Hu, Instrumental analysis, 4th ed, Higher Education Press, Beijing, 2008.

[30] J. G. Xu, Z. B.Wang, Fluorescence Analysis, 3rd ed, Science Press，Beijing, 2006.

[31] W. M. Yan,Q .Y. Wang, Q. Lin, M. Y. Li, J. L. Petersen, X. D. Shi, N-2-Aryl-1,2,3-triazoles: a novel class of UV/Blue-light-emitting fluorophores with tunable optical properties, Chem. Eur. J. 17 (2011) 5011-5018.

[32] V. Tekuri, D. R. Trivedi, A new colorimetric chemosensors for Cu^{2+} and Cd^{2+} ions detection: Application in environmental water samples and analytical method validation, Anal. Chim. Acta 972 (2017) 81-93.

[33] Zhang J., Yu C.W., Qian S.Y., etal. A selective fluorescent chemosensor with 1, 2, 4-triazole as subunit for Cu (II)and its application in imaging Cu (II) in living cells, Dyes Pigments 92 (2012) 1370-1375.

[34] K. Shah, N. Ain, F. Ahmed, I. Anis, M. R. Shah, A new highly selective chemosensor for the detection of iron ion in aqueous medium based on click generated triazole, Sensor Actuat. B 249 (2017) 515-522.

[35] C. Wu, Y. Ikejiri, J. L. Zhao, X. K. Jiang, X. L. Ni, X. Zeng, C. Redshaw, T. Yamato, A pyrene-functionalized triazole-linked hexahomotrioxacalix[3]arene as a fluorescent chemosensor for Zn^{2+} ions, Sensor Actuat. B 228 (2016) 480-485.

[36] W. Q. Che，G. Y. Jin,. Synthesis and biological activity of substituted carbamates and hydrzines containing bicyclophosphate, Chinese J. Applied Chem. 17 (2000) 479-482.

[37] X. Chen, T. Pradhan, F. Wang, J. S. Kim, J. Yoon, Fluorescent chemosensors based on spiroring-opening of xanthenes and related derivatives, Chem. Rev. 112 (2012) 1910-1956.

[38] F. Y. Yan, T. C. Zheng, D. C. Shi, Y. Zou, Y. Wang, M. M. Fu, L. Chen, W. G. Fu, Rhodamine-aminopyridine based fluorescent sensors for Fe^{3+} in water: synthesis, quantum chemical interpretation and living cell application, Sensor Actuat. B 215 (2015) 598-606.

[39] C. C. Jiang, M. Wang, Y. X. Wangc, X. N. Tang, Y. M Zhang, H. Zhang, L. Ma,J. Y. Wang, Synthesis and evaluation of two novel rhodamine-based fluorescence probes for specific recognition of Fe^{c+} ion, Tetrahedron Lette. 58 (2017) 2560-2565.

[40] E.J. Olson, P. Buhlmann, Getting more out of a job plot: determination of reactant to product stoichiometry in cases of displacement reactions and n:n complex formation, J. Org. Chem. 76 (2011) 8406-8412.

[41] Y. M. Yang, Q. Zhao, W. Feng, Fuyou Li, Luminescent Chemodosimeters for Bioimaging, Chem. Rev.113 (2017) 192-270.

[42] D. G. Cho, J. L. Sessler, Modern reaction-based indicator systems, Chem. Soc. Rev. 38 (2009) 1647-1662.

[43] X. Chen, T. Pradhan, F. Wang, J.S. Kim, J. Yoon, Fluorescent chemosensors based on spiroring-opening of xanthenes and related derivatives, Chem. Rev. 112 (2012) 1910-1956.

[44] J. L. Li, G. H. Ding, Y. Y. Niu, L. Y. Wu, H. J. Feng, W. Y. He, The structural properties of 5-methyl-2-phenyl -2H-1,2,3 -triazole-4-carboxylic acid and chromogenic mechanism on its rhodamine B derivatives to Hg^{2+} ions，Spectrochim. Acta Part A. 200 (2018) 127-135.

[45] Y. L. Lv, L. L. Zhu, H. Liu, Y. S. Wu, Z. L. Chen, H. B. Fu, Z. Y. Tian. Single-fluorophore-based fluorescent probes enable dual-channel detection of Ag+ and Hg2+ with high selectivity and sensitivity, Anal. Chim. Acta 839 (2014) 74-82.

[46] R. C. Gupta, S. S. Razi, R. Ali, S. K. Dwivedi, P. Srivastava, P. Singh, B. Koch, H. Mishra, A. Misra. An efficient Hg2+ ensemble based on a triazole bridged anthracene and quinoline system for selective detection of cyanide through fluorescence turn-off–on response in solution and live cell, Sensor Actuat. B 251(2017) 729-738.

[47] S. R. Bhatta, V. Bheemireddy, G.Vijaykumar, A. Thakur. Triazole appended mono and 1,1′ di-substituted ferrocene-naphthalene conjugates: Highly selective and sensitive multi-responsive probes for Hg(II), Sensor Actuat. B 240(2017) 640-650.

[48] J. D. Wu, J. R. Lu, J. G. Liu, C. H. Zheng, Y. X. Gao, J. Hu, Y. Ju. A deoxycholic acid-based macrocycle: Recognition of mercury ion and cascade enantioselective sensing toward amino acids, Sensor Actuat. B, 241(2017) 931-937.

[49] L. Y. Wang, G. P. Fang, D.C. Ye, D. R. Cao. Carbazole and triazole-containing conjugated polymer as a visual and fluorometric probe for iodide and mercury, Sensor Actuat. B 195(2014) 572-580.

[50] N. J. Wang, C. M. Sun, W. S. Chung A specific and ratiometric chemosensor for Hg^{2+} based on triazole coupled ortho-methoxyphenylazocalix[4]arene, Tetrahedron 67(2011) 8131-8139.

[51] D. Mandal, A. Thakur, S. Ghosh. A triazole tethered triferrocene derivative as a selective chemosensor for mercury(II) in aqueous environment, Polyhedron 52 (2013) 1109.

[52] Q. Y. Cao, Y. M. Han, H. M. Wang, Y. Xie. A new pyrenyl-appended triazole for fluorescent recognition of Hg2+ ion in aqueous solution, Dyes Pigments 99(2013) 798-802.

[53] M. Sulak, A. N. Kursunlu, B. Girgin, Ö. Ö. Karakuş, E. Güler. A highly selective fluorescent sensor for mercury (II) ion based on Bodipy and Calix[4]arene bearing triazolenaphthylene groups; synthesis and photophysical investigations, J. Photoch. Photobio. A 349 (2017) 129-137.

[54] B. Moosavi, B. Mousavi, W. C. Yang, G. F. Yang,Yeast-based assays for detecting protein-protein/drug interactions and their inhibitors, Eur. J. Cell Biol. 96 (2017) 529-541.

[55] B. Liu, X. M. Bi, L. McDonald, Y. Pang, D. Q. Liu, C. J. Pan, L. Wang, Solvatochromic fluorescent probes for recognition of human serumalbumin in aqueous solution: Insights into structure-propertyrelationship, Sensor Actuat. B 236 (2016) 668-674.

[56] Arabinda Mallick, Subhash Chandra Bera, Subhendu Maiti, Nitin Chattopadhyay, Fluorometric investigation of interaction of 3-acetyl-4-oxo-6,7-dihydro-12H indolo-[2,3-a] quinolizine with bovine serum albumin, Biophys. Chem. 112 (2004) 9-14.

[57] P. D. Ross, S. Subramanian, Thermodynamics of protein association reactions: forces contributing to stability, Biochemistry 20 (1981) 3096-3102.

[58] L. Stryer, Fluorescence energy transfers as a spectroscopic ruler. Annu. Rev. Biochem. 47 (1978) 819-846.

[59] L. Cyril, J. K. Earl, W. M. Sperry. Biochemists Handbook. London: E & FN Epon Led. Press, 1961.

[60] H. W. He, J. Zhang, H. M. Zhou, Y. B. Yan, Conformational changes in the C-terminal domain is responsible for the initiation of creatine kinase thermal aggregation, Biophys. J. 89 (2005) 2650-2658.

[61] A. O. Tiroli-Cepeda, T. B. Lima, T. S. Balbuena, F. C. Gozzo, C. H.I. Ramos, Structural and functional characterization of the chaperone Hsp70 from sugarcane. Insights into conformational changes during cycling from cross-linking/mass spectrometry assays, J. Proteomics 104 (2014) 48-56.

[62] M. S. Xiao, L. N. Han, L. Zhou, Y. H. Zhou, Comparison and investigation of bovine hemoglobin binding to dihydroartemisinin and 9-hydroxy -dihydroartemisinin: Spectroscopic characterization. Spectrochim. Acta, Part A 125 (2014) 120-125.

[63] K. Q. Wang, D. W. Sun, H. B. Pu, Q. Y. Wei, Principles and applications of spectroscopic techniques for evaluating food protein conformational changes: A review, Trends Food Sci.Tech. 67 (2017) 207-219.

[64] J. N. Miller, Recent advances in molecular luminescence analysis, Proc, Anal. Div. Chem. Soc. 16 (1979) 203-208.

[65] V. Bernard, Molecular Fluorescence: Principles and Applications, New York: Wiley-VCH, 2001.

[66]X. J. Guo, X. Z. Li, Y. C. Jiang, L. Yi, Q. Wu, H. C. Chang, X. Diao, Y. Sun, X. T. Pan, N. N. Zhou, A spectroscopic study on the interaction between p-nitrophenol and bovine serum albumin, J. Lumin. 149 (2014) 353-360.

[67] F. S. Mohseni-Shahri , M. R. Housaindokht , M. R. Bozorgmehr , A. A. Moosavi-Movahedi, The influence of the flavonoid quercetin on the interaction of propranolol with human serum albumin: Experimental and theoretical approaches, J. Lumin. 154 (2014) 229-240.

[68] J. R. Lakowicz, Principles of Fluorescence Spectroscopy, Plenum, New York, 1983.

[69] A. Samanta, B. K. Paul, N. Guchhait, Spectroscopic probe analysis for exploring probe–protein interaction: A mapping of native, unfolding and refolding of protein bovine serum albumin by extrinsic fluorescence probe. Biophys. Chem. 156 (2011) 128-139.

[70] M. X. Xie, M. Long, Y. Liu, C. Qin,Y. D. Wang,Characterization of the interaction between human serum albumin and morin, Biochim. Biophys. Acta Gen. Subj. 1760 (8) (2006) 1184-1191.

[71] N. A. Kratochwil, W. Huber,F. Müller, M. Kansy, P. R. Gerber, Predicting plasma protein binding of drugs: a new approach, Biochem. Pharmacol. 64 (2002) 1355-1374.

[72] G. Sudlow, D. Birkett, D. Wade, Further characterization of specific drug binding sites on human serum albumin, Mol. Pharmacol. 12 (1976) 1052-1061.

[73] F. Shiri, S. Shahraki, A. Shahriyar, M. H. Majd, Exploring isoxsuprine hydrochloride binding with human serum albumin in the presence of folic acid and ascorbic acid using multispectroscopic and molecular modeling methods, J. Photochem. Photobiol.B: Biology 170 (2017) 152-163.

[74] C. Qin, M. X. Xie, Y. Liu, Characterization of the Myricetin-Human Serum Albumin Complex by Spectroscopic and Molecular Modeling Approaches, Biomacromolecules 8 (2007) 2182-2189.

[75] W. S. Tao, W. Li, Y. M. Jiang, The Basic of Protein Molecules, 2nd ed, Higher Education Press, Beijing, 1995.

[76] S.Y. Jiang, L.Y. Zhang, Immunochemistry, Shanghai Medical University Press, Shanghai, 1996.

[77] S. C. Huang, E. S. Petersom, C. Ho, J. M. Friedman, Quaternary structure sensitive tyrosine interactions in hemoglobin: a UV resonance Raman study of the double mutant rHb (β99Asp→Asn, α42Tyr→Asp), Biochemistry 36 (1997) 6197-6206.

[78] A. L. Lehninger, D. L. Nelson, M. M. Cox, Principles of Biochemistry, second ed., CBS Publishers and distributors, India, 1993.

[79] R. K. R. Tummala, L. Chan, X. X. Guo, M. F. Peter, V. D. Lodewijk, Design, synthesis and SAR exploration of tri-substituted 1,2,4-triazoles as inhibitors of the annexin A2-S100A10 protein interaction, Bioorg. Med. Chem. 22 (2014) 5378-5391.

[80] S. L. Zhang, J. J. Chang, G. L.V. Damu, B. Fang, X. D. Zhou, R. X. Geng, C. H. Zhou, Novel berberine triazoles: Synthesis, antimicrobial evaluation and competitive interactions with metal ions to Human Serum Albumin. Bioorg. Med. Chem. Lett. 23(2013) 1008-1012.

[81] M. Gao, J. Ren, K. K. Tian, L. Y. Jia, Characterization of non-specific protein adsorption induced by triazole groups on the chromatography media using Cu (I)-catalyzed alkyne-azide cycloaddition reaction for ligand immobilization, J. Chromatogr. A 1476 (2016) 63-68.

[82] J. S. Lv, X. M. Peng, B. Kishore, C. H. Zhou, 1,2,3-Triazole-derived naphthalimides as a novel type of potential antimicrobial agents: synthesis, antimicrobial activity, interaction with calf thymus DNA and human serum albumin, Bioorg. Med. Chem. Lett., 24(2014) 308-313.

[83] D. Q. Chen, Y. H. Chen, F. L. Lian, L. Chen, Y. L. Li, D. Y. Cao, X. Wang, L. Chen, J. Li, T. Meng, M. Huang, M. Y. Geng, J. K. Shen, N. X. Zhang, B. Xiong, Fragment-based drug discovery of triazole inhibitors to block PDEδ-RAS protein-protein interaction, Eur. J. Med. Chem., 163 (2019) 597-609.

The specific binding of a new 1,2,3-triazole to three blood proteins and it's appended rhodamine complex for selective detection of Hg^{2+}

Guohua Ding[a], Luyong Wu[a], Huajie Feng[a], Yanping Liu[a], Jianling Li[a], Hongzong Si [b], Xiaojun Yao[c], Mengxiong He [a] , Wenying He [a]*

[a] *Key Laboratory of Tropical Medicinal Resource Chemistry of Ministry of Education, Hainan Normal University, 571158 Haikou, China*

[b] *Institute for Computational Science and Engineering, Qingdao University, 266071 Qingdao, China*

[c] *College of Chemical and Chemical Engineering, Lanzhou University, 730000 Lanzhou, China*

Highlights

- A synthesized 1, 2, 3-triazole EDTC was designed and synthesised a novel rhodamine based fluorescent chemosensors (REDTC).
- REDTC selectively responds to Hg^{2+} and also facilitates "naked-eye" detection of Hg^{2+}.
- Using chemometrics to analyze of the structural and photophysical properties of EDTC.
- Binding properties and parameters of EDTC to HSA, HIgG or BHb established based on molecular docking and the muti-spectral methods.

*Corresponding author at: Key Laboratory of Tropical Medicinal Resource Chemistry of Ministry of Education, Hainan Normal University, Hainan Normal University, Haikou 571158, China.
E-mail address: hewenying@hainnu.edu.cn(WY He)

Disclosure statement

The authors have declared no conflict of interest.